EFFECT OF NON-CONDENSABLE GASES ON THE ADSORPTION PROPERTIES OF ADSORBENT POROUS MEDIA

A THESIS SUBMITTED TO
THE GRADUATE SCHOOL OF NATURAL AND APPLIED SCIENCES
OF
MIDDLE EAST TECHNICAL UNIVERSITY

BY

ORHAN ATA BAYMAN

IN PARTIAL FULFILLMENT OF THE REQUIREMENTS
FOR
THE DEGREE OF MASTER OF SCIENCE
IN
MECHANICAL ENGINEERING

DECEMBER 2014

Approval of the thesis:

EFFECT OF NON-CONDENSABLE GASES ON THE ADSORPTION PROPERTIES OF ADSORBENT POROUS MEDIA

submitted by **ORHAN ATA BAYMAN** in partial fulfillment of the requirements for the degree of **Master of Science in Mechanical Engineering Department, Middle East Technical University** by,

Prof. Dr. Gülbin Dural Ünver _____
Dean, Graduate School of **Natural and Applied Sciences**

Prof. Dr. Tuna Balkan _____
Head of Department, **Mechanical Engineering**

Assoc. Prof. Dr. Cemil Yamalı _____
Supervisor, **Mechanical Engineering Dept., METU**

Examining Committee Members:

Prof. Dr. Kahraman Albayrak
Mechanical Engineering Dept., METU _____

Assoc. Prof. Dr. Cemil Yamalı
Mechanical Engineering Dept., METU _____

Assoc. Prof. Dr. Derek K. Baker
Mechanical Engineering Dept., METU _____

Assoc. Prof. Dr. İlker Tarı
Mechanical Engineering Dept., METU _____

Prof. Dr. Atilla Bıyıkoğlu
Mechanical Engineering Dept., Gazi University _____

Date: _____

I hereby declare that all information in this document has been obtained and presented in accordance with academic rules and ethical conduct. I also declare that, as required by these rules and conduct, I have fully cited and referenced all material and results that are not original to this work.

Name, Last Name: ORHAN ATA BAYMAN

Signature :

ABSTRACT

EFFECT OF NON-CONDENSABLE GASES ON THE ADSORPTION PROPERTIES OF ADSORBENT POROUS MEDIA

Bayman, Orhan Ata

M.S., Department of Mechanical Engineering

Supervisor : Assoc. Prof. Dr. Cemil Yamalı

December 2014, 84 pages

Non-condensable gases such as air can penetrate into adsorption machines that utilize adsorbates which work at negative gage pressures. As many adsorption cooling/heat pump applications involve such negative gage pressures, it becomes important to research the effects of such non-condensable gases on the adsorption properties. In this thesis, prescribed amounts of air have been injected into an experimental apparatus containing an adsorbent bed and an evaporator/condenser to observe the effects of air on the adsorption and desorption properties of natural zeolite-water, Zeolite 13X-water and silica gel-water adsorbent-adsorbate pairs, respectively. These different amounts of air have been tested at various evaporater/condenser and adsorbent temperatures. Adsorption and desorption processes were started by lowering and raising the adsorbent temperature to certain temperatures while at equilibrium with evaporator/condenser, respectively. Temperature of evaporator/condenser was held constant during that process. Comparisons are made between experiments with different air amounts, evaporator/condenser temperatures and desorption-adsorption working temperatures. Adsorption and desorption capacities and their reductions from no-air experiments, changes in gas (vapor and air) pressure, gas temperature and average adsorbent temperature over time are tabulated. Significant reductions in both final adsorption and desorption capacities have been observed with increasing amounts of air for all adsorbents, which will affect the cooling and heating capacity of an adsorp-

tion refrigerator/heat pump. Both adsorption and desorption capacities reduced less at higher evaporator/condenser temperatures for the same amount of air. Decay in adsorption capacity has been found to be logarithmic for zeolites and exponential for silica gel. Experiment with lower difference between desorption-adsorption temperatures has been found to be more affected than a higher one for the same amount of air. Desorption capacities have been found to be more affected by the presence of air. Hysteresis also increased with increasing amounts of air. It is concluded that precautions should be taken very seriously for avoiding penetration of air into an adsorption machine as only a small amount of residual air (0.3-0.9% of atmospheric pressure) can drastically reduce the adsorption and desorption performance.

Keywords: Solar cooling, Adsorption refrigeration, Adsorption cooling, Adsorption heat pump, Non-condensable gas, Non-adsorbable gas, Residual air, Natural zeolite, Silica gel, Zeolite 13X

ÖZ

YOĞUŞAMAZ GAZLARIN GÖZENEKLİ ADSORBAN MADDENİN ADSORPSİYON ÖZELLİKLERİ ÜZERİNDEKİ ETKİSİ

Bayman, Orhan Ata
Yüksek Lisans, Makina Mühendisliği Bölümü
Tez Yöneticisi : Doç. Dr. Cemil Yamalı

Aralık 2014 , 84 sayfa

Hava gibi yoğuşamaz gazlar negatif göreli basınçlarda çalışan adsorpsiyon makinalarının içine sızabilmektedirler. Birçok adsorpsiyon soğutma/ısı pompası uygulaması negatif göreli basınçlarda çalıştığından dolayı, yoğuşamaz gazların adsorpsiyon özelliklerine etkilerinin araştırılması önem kazanmaktadır. Bu tezde, önceden belirlenen hava miktarları, doğal zeolit-su, Zeolit 13X-su ve silika jel-su adsorban-adsorbat çiftlerinin adsorpsiyon ve desorpsiyon süreçlerine havanın yarattığı etkileri incelemek için bir adsorban yatağı ve bir evaporatör/kondensörden oluşan bir deney düzeneğine enjekte edilmiştir. Değişen hava miktarları, değişik evaporatör/kondensör ve değişik adsorban sıcaklıklarıyla test edilmiştir. Adsorpsiyon ve desorpsiyon süreçleri, evaporatör/kondensör ile denge halindeyken, sırasıyla adsorbanın sıcaklığının belli sıcaklıklara düşürülmesi ve çıkarılması yoluyla başlatılmıştır. Evaporatör/kondensör sıcaklığı bu süreç boyunca sabit tutulmuştur. Farklı hava miktarları, evaporatör/kondensör sıcaklıkları ve desorpsiyon-adsorpsiyon çalışma sıcaklıklarında çalışan deneyler arasında karşılaştırmalar yapılmıştır. Adsorpsiyon ve desorpsiyon kapasiteleri ve havasız deneylere göre düşme miktarları, gaz (buhar ve hava) basıncı, gaz sıcaklığı ve ortalama adsorban sıcaklıklarının zamana göre değişimleri gösterilmiştir. Hava miktarının artmasıyla beraber son adsorpsiyon ve desorpsiyon kapasitelerinde önemli miktarda düşüş gözlenmiştir. Bu düşüşler, adsorpsiyon soğutma veya ısı pompalarının soğutma/ısıtma kapasitelerinde düşüşe neden olacaklardır. Hem adsorpsiyon hem desorp-

siyon kapasitelerindeki düşüş, aynı hava miktarları için, yüksek evaporatör/kondensör sıcaklıklarında daha az gözlenmiştir. Adsorpsiyon kapasitelerindeki düşüş, zeolitler için logaritmik, silika jel için eksponansiyeldir. Aynı miktarda hava için, düşük desorpsiyon-adsorpsiyon sıcaklık aralığındaki deney, yüksek sıcaklık aralığındakine göre adsorpsiyon kapasitesinde daha fazla düşüş göstermiştir. Desorpsiyon kapasiteleri havanın varlığından daha fazla etkilenmişlerdir. Histerezis de hava miktarının artmasıyla artmıştır. Bu tezin sonucunda, hava sızdırmalarına karşı alınacak önlemlerin oldukça ciddiye alınmalarının gerekliliği sonucuna ulaşılmıştır; nitekim çok az miktarda hava bile (%0.3-0.9 atmosferik basınç) adsorpsiyon ve desorpsiyon performansını derinden etkileyebilmektedir.

Anahtar Kelimeler: Güneş enerjisiyle soğutma, Adsorpsiyon soğutma, Adsorpsiyon serinletme, Adsorpsiyon ısı pompası, Yoğuşamaz gaz, Adsorbe olamaz gaz, Artık hava, Doğal zeolit, Silika jel, Zeolit 13X

To my family and friends

ACKNOWLEDGMENTS

Firstly, I would like to thank my adviser Assoc. Prof. Cemil Yamalı, for, apart from his scientific assistances, his kind personality. For behaving me not as a subordinate like many, but rather, as a colleague. I would also like to thank Mustafa Yalçın, our technician in the heat transfer lab. Without his help, I could never get my experiment set up. He helped me with even the slightest problem and malfunction I had encountered, not just out of obligation and grumbling about it, but by his instinctive motivation of fixing things and liking it.

M.D. Emel Sönmez has my special thanks. Without her assistance, this thesis might never be finished at all. She gave me a new insight, a new perspective to the way I look to my life.

I would also like to mention Ivan Glaznev, Daniil Ovoshchnikov and Yuri Aristov for their work. Their study on the effects of residual air on adsorption had become a stepping stone for my work. I appreciate them for conducting an experimental study on this subject, which is otherwise a barren topic of interest.

I would specifically like to mention all my friends, dormitory mates and all people who had entered my life in this three year period. My gratitudes to, in order of acquaintance: Serkan Özen, Fatih Yılmaz, Ahmed Abbas Momin, Sina Khoshsima, Mustafa Usman and Serhat Özdemir. If I have written half of this thesis myself, you have written the other half. All the joy and suffering, good and bad, I shall remember.

Finally, I want to mention my dearest family. Ali Bayman, my father, for always encouraging me when I was down and for always supporting me when I was up. Without his assistance, morally and financially, an M.S. degree was not probable. Zeynep Çakır, my mother, for always believing in me, without a second thought. She has ever valued me and will continue to do so, regardless of whatever I have become and whatever I will become. Although she will probably not see her house being called “a professor’s house” as my career plans do not involve a Ph.D. for now, I am delighted that I granted her wish of becoming a ‘senior’ engineer, not a ‘junior’ one.

TABLE OF CONTENTS

LIST OF TABLES

TABLES

LIST OF FIGURES

FIGURES

LIST OF ABBREVIATIONS

BSL	best straight line
COP	coefficient of performance
D	inner diameter of evaporator/condenser, m
D_{stick}	diameter of metal stick that is carrying thermocouples within evaporator/condenser, m
E	reading error of adsorption and desorption capacities
$E_{d/a\ upper}$	upper reading error of desorption to adsorption capacity ratio, %
$E_{d/a\ lower}$	lower reading error of desorption to adsorption capacity ratio, %
FS	full span
m_{ads}	dry mass of adsorbent, kg
P_A	partial air pressure, mbar
P_{gas}	gas pressure, mbar
P_{res}	residual pressure within pipeline, mbar
P_{tot}	total pressure within pipeline, mbar
P_W	partial vapor pressure, mbar
Red.	reduction by percentage, %
T_{ads}	average adsorbent temperature, °C
T_{gas}	gas temperature, °C
T_{sat}	saturation temperature of adsorbate, °C
VC	vapor-compression
W_{th}	thermal work, J
X_{ads}	adsorption capacity
X_{des}	desorption capacity
ΔL	difference in water level, m
ρ_{water}	density of liquid water at evaporator/condenser temperature, kgm^{-3}

CHAPTER 1

INTRODUCTION

1.1 ADSORPTION REFRIGERATION SYSTEMS

The world's energy demand is increasing along with developing industry and increasing population. Internal Energy Agency predicts an increase of 35 percent in world's energy demand by the year 2035 [1]. Part of this energy demand comes from the desire to generate cooling power. The practice of carrying heat from low temperature region to a hot one is utilized throughout the world from air conditioning to refrigeration. Most of this demand today is met with a mechanical input by a compressor mostly driven by electrical power; the vapor-compression (VC) cycle. VC refrigerators are dominating the refrigeration market so much that in 2005, 99.9% of all refrigerators delivered in United States were VC based. This is due to their low capital cost, high coefficient of performance and good personal safety record. However, such dependence on electricity puts significant stress on electricity generation. As an example, space cooling and refrigeration only, consumed 24.8% of total electricity consumption in United States [2]. 15% of all electricity produced in the world is consumed on refrigeration and air-conditioning [3]. A novel method, absorption and adsorption cooling systems started to take place mainly where excess heat or solar energy is available. Adsorption is the phenomenon of the adhesion of molecules, atoms or ions of a substance or substances onto a surface, which is in practice, mainly a porous media. Adsorption of molecules cause a pressure drop within surrounding fluid. This, in turn provides cooling by evaporation of refrigerant liquid and thus, removing latent heat. This is how an adsorption cooler works at its simplest. Adsorbing, solid part of this phenomena is called 'adsorbent'. Adsorbed, fluid part is called

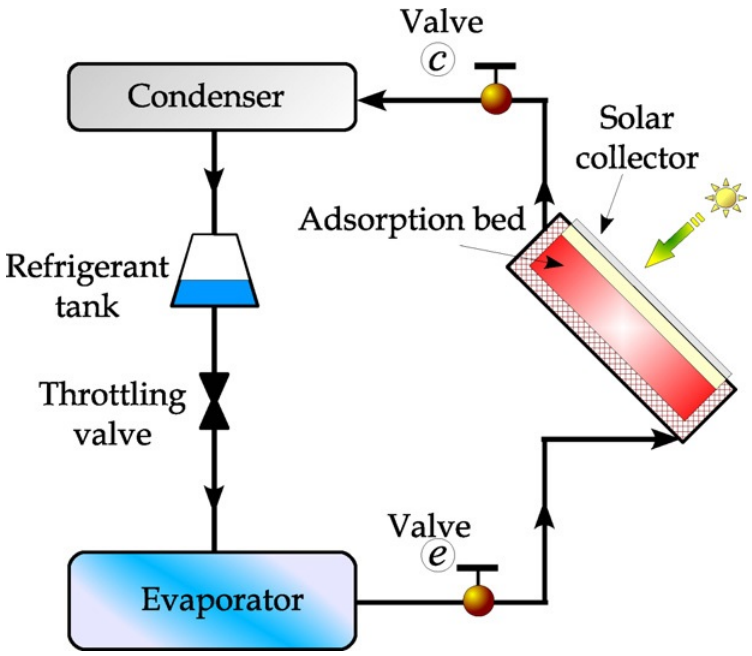

Figure 1.1: Diagram of a typical solar adsorption cooling machine [5].

'adsorbate'. Absorption, on the other hand is the permetion of an absorbate fluid into an absorbent fluid or solid phase, effectively forming a solution. So, while absorption describes a volumetric process; adsorption describes a surface-based process. Absorption and adsorption are phenomenons long known by science and utilized by engineers; it was first discovered by Michael Faraday in 1848 as ammonia was adsorbed on AgCl [4]. However the utilization of such phenomenons in refrigeration or heat-pump applications are relatively new. Such refrigerators operate similarly to a VC one, except heat is the prime mover instead of mechanical power.

1.1.1 Advantages and Disadvantages

Adsorption phenomenon has already been thoroughly used in many other fields of industry such as gas-seperation, desalination and water purification. Their cooling applications are being relatively recently developed and studies are conducted as the process posseses some advantages over vapor-compression refrigerators. One of the main advantages of adsorption refrigeration to vapor-compression refrigeration is about anthropogenic environmental impact. Apart from using heat as the driving power, adsorption chillers are free of common refrigerants: CFC (Chlorofluorocarbons) such as R-12 and HCFC (Hydrochlorofluorocarbons) such as R-21 un-

like traditional vapor-compression chillers [2]. Aforementioned materials have many side-effects to both environment and human health. Ozone depletion, contribution to global warming and toxicity are such examples. Adsorption systems generally use environmentally benign and easily found materials like water. This, in turn, reduces the effects of aforementioned gases on environment.

Adsorption chillers utilize heat instead of electricity. They are specifically capable of using low-temperature heat. Comparing to absorption and thermo-mechanical ejector cycles, adsorption cycles are operated at lower regeneration temperatures [1]. Thus, they are ideal for usage where geothermal and especially solar thermal energy is available. Adsorption systems also possess other advantages over absorption coolers. They can work with higher temperature heat sources without corrosion, whereas corrosion starts above 200°C for absorption systems. Adsorption coolers are also more robust in vibrating conditions, ideal for vehicle applications. As absorption is a fluid-fluid system, flow can occur from absorber to condenser and from generator to evaporator, effectively polluting the refrigerant. An adsorption system is also simpler to design; certain working pairs of absorption may require additional equipment [6]. It was also found that adsorption systems are more suitable for small-scale air conditioning systems, whereas absorption systems are more suited to large-scale building air conditioners [7]. All being said, absorption coolers still have higher performance than adsorption ones. Thermo-mechanical ejector systems have the highest COP's, but they also need higher temperature heat sources [8].

Adsorption systems can also be utilized in combination with power systems. Those efficient systems are called combined cooling heating and power systems (CCHP). Heat, which emerge as a byproduct of electricity generation in a power generation unit, can be used in a sorption chiller for cooling demands [4, 9, 10].

Many households today utilize modest-sized solar thermal energy systems which generates excess heat especially during hot summer months with higher solar irradiation. This readily available heat can easily be used in an adsorption chiller as a complement or even an alternative to traditional vapor-compression refrigerators by means of heat storage. Unlike the compressor of vapor-compression chiller or the compressor-turbine couple of a Brayton refrigerator, adsorption chillers use minimal

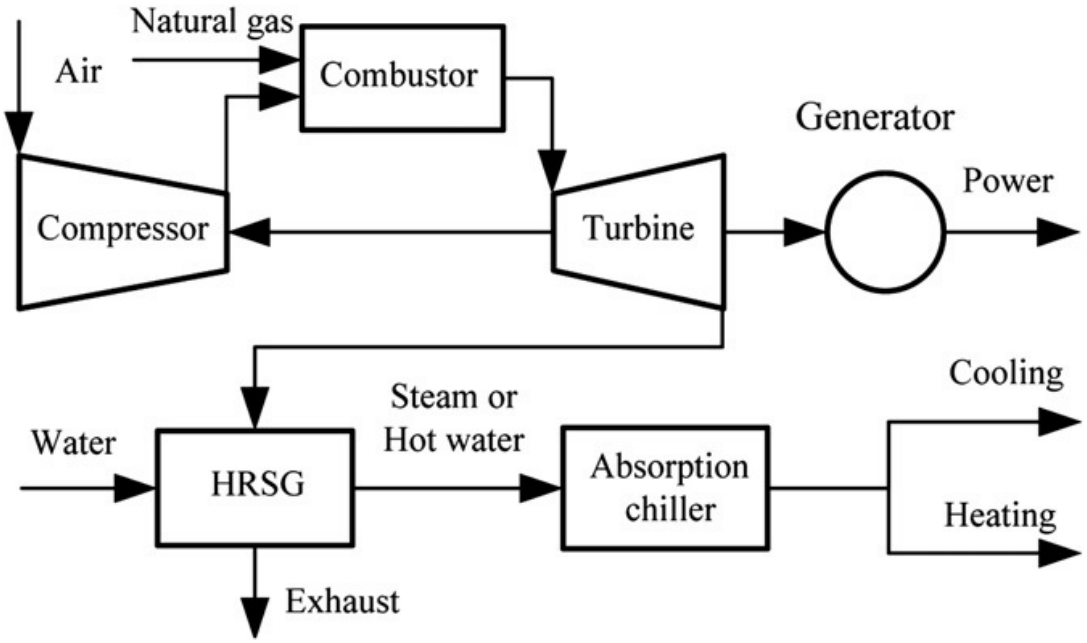

Figure 1.2: Diagram of a typical CCHP system with an absorption chiller [10].

to none moving parts. Those moving parts generally tend to be ubiquitous and relatively easily maintained pumps and valves. They also work quieter. Materials used in adsorption chiller are relatively easily attainable and transferable such as zeolite, silica gel, activated carbon and activated alumina as adsorbents and water, methanol and ammonia as adsorbates.

There are also many hindrances for adsorption refrigeration to be widespread. Adsorpion refrigerators typically suffer from low COPs, maintenance issues, pressure drop, and the need for a heat source to regenerate the adsorbent [2]. For example, one of the most popular working pairs operating at lower temperatures, silica gel-water is plagued by low heat and mass transfer performance resulting in large size, low performance and high costs [11]. Weak heat and mass transfer performance of adsorption is said to create a barrier for further improvement of this technology. However, studies are conducted to overcome this problem [12]. Besides those, solar thermal energy driven cycles in general, have lower overall energy conversion efficiencies, higher initial costs than electrically driven VC cycles and inherent discontinuity of solar irradiation [1]. However, heat storage methods exist in the form of the sensible heat of a solid or liquid, the latent heat of a phase changing substance, or by means of a chemical reaction. Cool thermal energy storage (CTES) is another form of heat storage, in which generated coolness is stored either in sensible or latent heat form.

Table 1.1: Coefficients of performance (COP) for adsorption, absorption with different working pairs and VC cycles [16].

Type of cycle	Working pairs	Coefficient of performance (COP)
Adsorption	Activated Carbon-Methanol	0.12–1.06
	Zeolite-Water	0.28–1.4
	Silica gel-Water	0.25–0.65
Absorption	Methanol-Water	0.7–1.1
	Lithium bromide-Water	
Vapor-compression (VC)		3–4

This type of storage requires better insulation as energy available in its cool state is more expensive [13]. Adsorption refrigerators are also larger [3]. Lower COP values remain the single most important disadvantage of adsorption systems. It was reported that COP values of sorption systems in general, range from approximately 0.1 to 1.7 [10]. Generally, depending on the driving heat's temperature, adsorption cooling cycles were said to achieve a COP between 0.3-0.7 [1]. COP's were reported at 0.10-0.12 for zeolite-water pairs, 0.05 for activated carbon-ammonia, and 0.2-0.3 for silica gel-water working pairs [8]. For a temperature lift of 20°C at room temperature with a heat source temperature of 600 K, ratio of actual COP values to that of Carnot cycle was found to be between 0.01 to 0.09 for adsorption [10]. In one instance [14], a COP as much as 1.19 was reported which is also the record for adsorption coolers but this result was never reproduced again [15].

Adsorption deterioration is another drawback for adsorption coolers, effectively reducing the service life [12]. Finally, as adsorbates like water and methanol work below atmospheric pressures, vacuum leakages present an important problem, which is also the topic of interest in this study. This study is devoted to investigate what possible side-effects might happen when controlled amounts of air are deliberately injected into an experimental adsorption system.

Commercially, two Japanese companies (Nishiyodo and Mycom) reported that ad-

sorption chillers better performed than absorption ones for lower-grade heat, although their reliability was disputed [15]. While comparing the economics of the various solar cooling methods, it was asserted that most economical ones were, respectively, photo-voltaic driven VC refrigerators, electrically driven VC refrigerators driven by stirling engine-parabolic dish couple, double-effect absorption cycle driven by concentrating trough collectors and desiccant systems driven by flat-plate solar collectors. Adsorption systems were found to be significantly more expensive [17].

1.1.2 Adsorption Refrigeration in Turkey

Proliferation of adsorption refrigeration is specifically important in Turkey. Turkey has a growing energy demand which is mainly supplied from imported natural gas, environmentally damaging lignite/hard coal or hydroelectric dams [18]. Turkey has a considerable output in terms of solar radiation. While solar energy is used minimally in terms of generating electricity in the country, many households and the tourism industry already utilize solar thermal energy in abundance for heating water. Previous studies in Mediterranean like climates already showed adsorption cooling to be promising in such areas [19]. With small amount of modifications, this readily available thermal energy can easily be used in an adsorption refrigeration system. At least some of this refrigeration power can be used in both refrigeration and air-conditioning. This would reduce the demand for electricity in places where solar thermal energy is readily available throughout the country, especially during summer months with inherent higher irradiation.

1.1.3 Future of Adsorption Refrigeration

While adsorption refrigeration cannot take place of vapor-compression refrigeration completely at least in foreseable future, it can and it is complementing the traditional refrigeration systems. It was assesed that while R&D will continue on such systems, they will not be widespread unless cost of primary energy sources significantly rise. However, they would tend to be used where management of peak electricity demand is important and where there are plenty of heat sources readily available both in low

and high temperature [2]. Studies are going on to utilize new types of adsorbents [20], using advanced cycles, enhancing heat and mass transfer [12]. Especially, application of nano-technology to produce new adsorbents may take adsorption cooling to a more cost competitive level. Hybrid systems are also considered for that reason: like adsorption with ejector refrigeration, adsorption with desiccant humidification and adsorption with thermoelectric cooling [21]. Fixed adsorbent beds may be replaced by fluidized bed technology, thus eliminating the inherent high heat and mass transfer resistances of fixed bed systems [3]. It was extrapolated that, by 2030, a 5-ton adsorption unit would cost \$1.14/$W_{th}$of cooling , same that of a Li-Br absorption unit. A same size NH_3 absorption unit would cost \$0.28/$W_{th}$of cooling and a desiccant unit would cost \$1.42/$W_{th}$of cooling [22].

1.2 PRINCIPLES OF ADSORPTION

Adsorption is the phenomenon of the adhesion of molecules, atoms or ions of a substance or substances onto a surface. The adhering phase is called 'adsorbate', whereas the solid surface being adhered onto is called 'adsorbent'. Adsorbent and adsorbate together create a 'working pair'. Adsorption capacities, working temperatures, working pressures, inherent side effects all differ from one pair to another. Adsorption capacity is basically the ratio of amount of adsorbate adsorbed by the adsorbent in terms of mass. Operating conditions of the application decides which working pairs should be used in an adsorption system, i.e. whereas silica gel work with low-grade heat, zeolites are more suitable for high temperature applications. Adsorption process is typically divided to two in terms of the bonds they make:

1. Physical Adsorption (Physisorption)
2. Chemical Adsorption (Chemisorption)

Physical adsorption involves binding by weak Van der Waals forces between adsorbent and adsorbate. It is also called as 'physisorption'. This is the type of adsorption process that is generally used in adsorption cooling systems as the process is reversible simply by applying heat to adsorbent. By applying heat, adsorbed molecules

loose free from their binding on the adsorbent. This process is called 'desorption', the reverse process of adsorption. Therefore, an adsorption refrigerator may work in a continous cycle of refrigerating adsorption and regenerative desorption processes. Some of popular physisorption working pairs are given below along with their characteristics at Table 1.2.

Chemical adsorption is the process where stronger covalent and ionic bonds form between adsorbent and adsorbate. This process is also known as 'chemisorption'. This process may not be completely reversible. Therefore they are generally not suitable for adsorption refrigeration. Some working pairs of chemisorption and their characteristics are given at Table 1.3. Hybrid systems are also devised for better cooling options. There are two purposes for that. One is to increase heat and mass transfer with a high thermal conductivity and a porous structure. Another is to increase adsorption capacity by adding chemical adsorbents to physical adsorbents [6].

As the adsorption process causes the adsorbate to lose heat by evaporation, heat is generated on adsorbent as a result adsorption. This heat is generally 30-100% higher than the latent heat of adsorbate due to condensation. The amount of heat generated can be determined either experimentally as differential heat of adsorption by means of a calorimeter or as isosteric heat of adsorption from adsorption isotherms. Adsorption isotherms are relations linking equilibrium adsorption capacity to adsorbate pressure and adsorbent temperature. They are important relations in a refrigerator design as adsorption capacities of an ideal cycle can be deduced from those equations for respective temperatures of adsorbate and adsorbent. As an example, Modified Dubinin-Astakhov isotherm equation for activated carbon-methanol is given in Equation 1.1.

$$X_{ads} = 0.45 exp\left[-13.38\left(\frac{T_{ads}}{T_{sat}} - 1\right)\right] \tag{1.1}$$

Adsorbents used in physisorption are mostly porous media. Therefore surface properties are an important part of adsorption performance.

Table 1.2: Common characteristics of some popular physisorption refrigeration working pairs [6].

Working pair (Adsorbent-Adsorbate)	Characteristics
Silica gel-Water	Good performance up to 200°C. Thus, COP decreases due to overheating issues. As latent heat of water is relatively high, it shows good performance. Water is also able to work at low temperatures.
Zeolite-Water	As the water has a freezing temperature of 0°C, pair is practical to use for air-conditioning. Zeolites can work at higher temperatures effectively, above 200°C. Specific cooling power can be increased (600W/kg) by using specific materials.
Activated carbon–Methanol	Largest COP is achieved with methanol as adsorbate Only applicable with temperatures below 120°C as methanol starts to decompose. Lower thermal conductivity results in acting as an insulator.
Activated carbon–Ammonia	The pair is characterized by larger working temperatures, good heat and mass transfer and high cooling capacity. Ammonia has about 2/3 of the adsorption capacity (0.29 kg/kg) comparing to that of methanol (0.45 kg/kg). Corrosion, outward leakage and toxicity are common issues. Ammonia can work in positive gage pressures.

Table 1.3: Common characteristics of some popular chemisorption refrigeration working pairs [6].

Working pair (Adsorbent-Adsorbate)	Characteristics
Metal chloride-Ammonia	Has a low boiling point. Can be utilized for ice production. Specific Cooling Power= 731 W/kg COP= 0.38
	Mixing with 20% $CaSO_4$can reduce agglomeration problem. Deterioration, expansion, decomposition and corrosion are common problems.
Metal hydrides-Hydrogen	Higher density and requires small spaces (6.5-8 kg/L).
	No saturated adsorbate. The cycle follows the hysteresis phenomenon.
Metal oxides-Oxygen	Using 2.85$m^3$of CaO within first hour at a temperature of 998°C allows to achieve 1 MW of energy.
	Nanoparticles (10 nm) can increase performance.

1.3 EFFECTS OF NON-CONDENSABLE GASES ON ADSORPTION PERFORMANCE

Many thermal powered adsorption cooling systems work below the atmospheric pressure, including water based systems. Non-condensable or non-adsorbable gases may be present within a thermal powered adsorption cooling system in some different ways. Partial evacuation, leakages or desorption from the adsorbent bed can cause air to be present within the system as a non-condensable. Air may be one of the most encountered non-condensable within an adsorption chiller as such. Hydrogen gas can also be present due to corrosion [24].

By nature, an adsorption process involves surface and intraparticle heat and mass transfer resistances. Presence of gases apart from the working fluid create extra heat and mass transfer resistances upon that, especially if such gases are non-adsorbable. As a result of this, presence of such gas or gases effectively reduce the rate of adsorption and specific cooling power, especially on the systems which utilize an adsorbate that works with negative gage pressures, like water. An explanation of such reduction is reported to be possibly tied to the Stephan flux [25, 26]. This flux creates a layer out of already present non-adsorbable gas on adsorptive surface. Adsorption is then governed by diffusion of adsorbate through that layer, effectively creating extra mass and heat transfer resistance on the adsorbent which is larger than the one possessing only surface and intraparticle resistances [24]. Accumulation of non-adsorbables within pores of the adsorbent also adds extra resistance as well. All of those phenomenas result in a reduction in rate of adsorption.

Many studies were conducted concerning the effects of non-condensables over condensation and absorption. Reduction of condensation rate due to presence of non-condensables was observed many times by different authors and is a well known phenomena [27, 28, 29, 30, 31]. Effects of non-absorbables on absorption are also well studied as well. About 50% of reduction in heat transfer in an absorption heat-pump was observed with existence of 50% concentration of air in water vapor [32]. Presence of only 5% concentration of non-absorbable gas was reported to cause 300% of reduction in absorption [33]. It was predicted that only 2% of air by concentration would be enough to reduce the coefficient of performance of an absorption refrigera-

tor to sixth of its original performance.

Effects of gas mixtures on adsorption in its gas separation usage is widely studied and utilized in many practical applications. However, their effects on heat-pump and refrigeration utilities of adsorption are relatively less studied and much of the literature that studied are mainly ancillary reports of negative effects of non-adsorbables. Generation of hydrogen is observed as a byproduct in chlorine production where it accumulates in a heat exchanger-condenser [34]. This results in a reduction in average chlorine concentration and accumulation of hydrogen near the condenser surface which is reported to be caused by Stephan flux [26, 35]. Presence of residual air was reported to reduce heat transfer in a granulated adsorbent bed and it was asserted that this effect can reduce the performance of an adsorption machine [35]. In reference to [36], it was asserted that evaporator and condenser heat rate can be reduced 50% by the presence of 1% to 2% non-condensable gases due to its effect on two-phase heat transfer. Systematic analysis on this topic were also done recently. In reference [24], effects of air upon kinetics of water adsorption on loose grains of the composite adsorbent SWS-1L (silica KSK modified by calcium chloride) [37] were investigated. Working temperatures were 60°C for desorption and 35°C for adsorption upon an isothermal metal plate at 10.3 mbar water vapor pressure and certain partial air pressures between 0 and 4.7 mbar. Adsorption stage was conducted almost isobarically. Reduction in adsorption rate was observed as low as 0.06mbar of partial air pressure. Above the partial air pressure of 0.4 mbar, kinetic curves were near-exponential and above 1mbar, characteristic adsorption time did not depend on the grain size and increased from the original. Desorption was found to be less affected by air. Specific cooling power was related as function of partial air pressure during isobaric adsorption stage. This study was further improved by testing two more adsorbents [38]. Those two adsorbents are silica Fuji type RD [39, 40] and FAM-Z02 [41]. Reduction in adsorption rate at air pressure as low as 0.06 mbar was observed again. Desorption stage was more resilient to air as well. Characteristic adsorption time related linearly with partial air pressure above 0.4 mbar with slope depending on the adsorbent type. The cooling power was found to be dramatically decreasing with increasing presence of air, indicating a high amount of sensitivity. Careful removal of air and vacuum drying of thermo-liable materials were highly recommended before startup

of an adsorption unit. With the same conditions that were used in experiments, a mathematical model of coupled heat and mass transfer in an adsorbent SWS-1L layer was conducted with air and hydrogen as non-adsorbables [42]. It was seen that adsorption of water by the adsorbent layer created a layer of non-adsorbable upon it by sweeping the non-adsorbable gases towards adsorbent due to momentum generated during adsorption of water. Similar results were obtained with that of experimental data. Even minute amount of air was observed to dramatically decrease effective heat transfer coefficient and slow down the adsorption and heat transfer processes. Effective heat transfer coefficient had reduced from 50-70 W/m^2K for pure vapor to 4 W/m^2K at P_A=1.0 mbar or P_A/P_W= 0.097.

CHAPTER 2

EXPERIMENTAL METHOD

2.1 DESCRIPTION OF THE EXPERIMENTAL SET-UP

A simple experimental setup for adsorption refrigeration is used to test the effects of air. Core of the test setup are an adsorbent bed which houses the adsorbent and a water filled evaporator/condenser. Both could be held at constant temperature. A schematic and photograph of this set-up can be seen in Figure 2.1 and Figure 2.2.

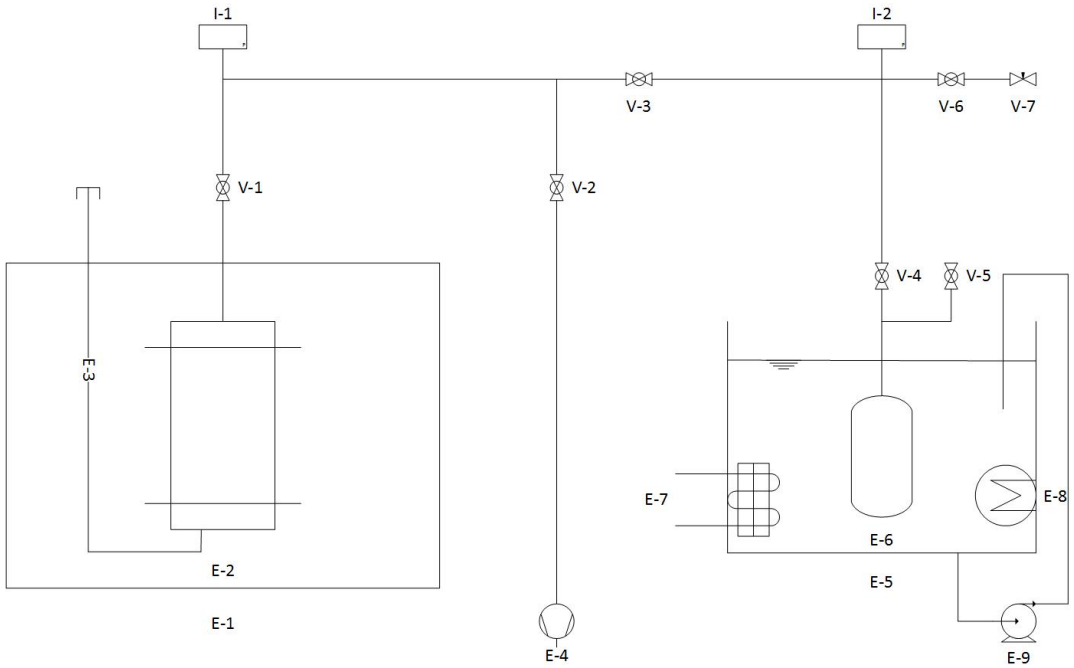

Figure 2.1: A schematic view of the experimental set-up (E-1 Oven; E-2 Adsorbent Bed; E-3 Thermocouple Output; E-4 Vacuum Pump; E-5 Water Bath; E-6 Evaporator/Condenser; E-7 VC Refrigeration Unit; E-8 Electrical Heater; E-9 Water Pump; I-1,2 Pressure Transducers; V-1 ... 6 Vacuum Ball Valves; V-7 Fine Valve).

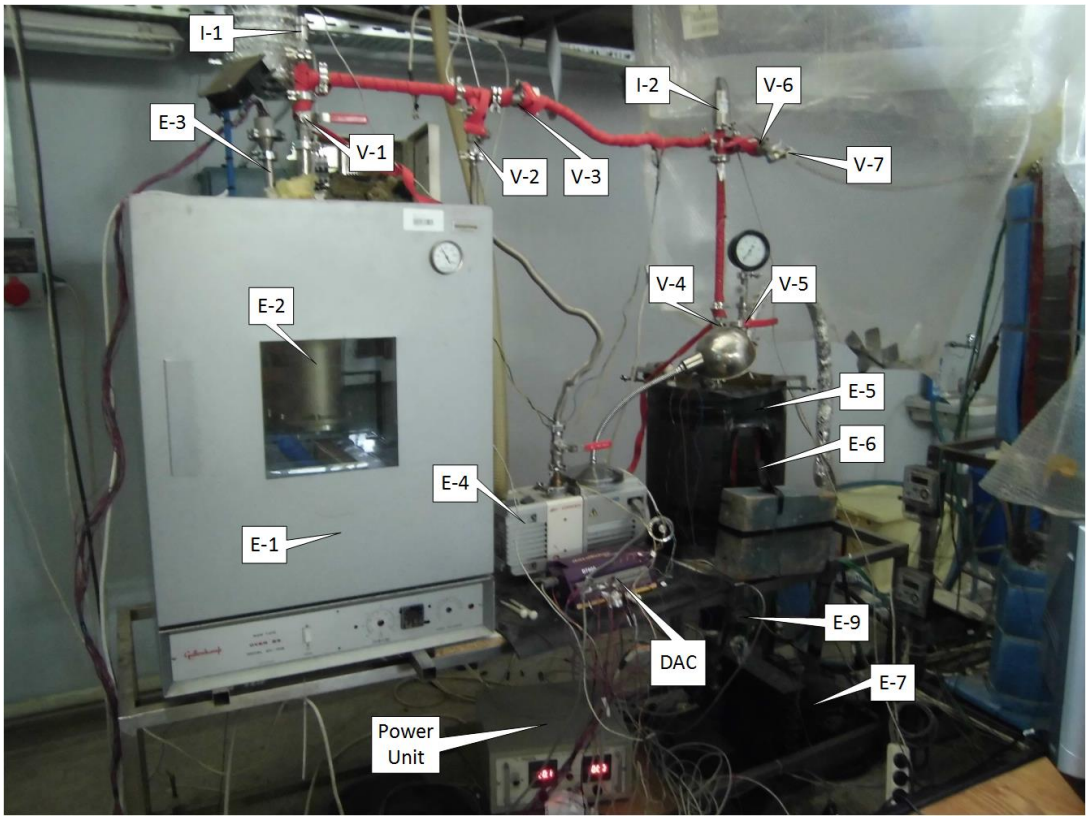

Figure 2.2: A photograph of the experimental set-up (E-1 Oven; E-2 Adsorbent Bed; E-3 Thermocouple Output; E-4 Vacuum Pump; E-5 Water Bath; E-6 Evaporator/Condenser; E-7 VC Refrigeration Unit; E-9 Water Pump; I-1,2 Pressure Transducers; V-1 ... 6 Vacuum Ball Valves; V-7 Fine Valve; DAC: Data Acquisition and Control).

2.1.1 Adsorbent Bed

The adsorbent bed is a 250 mm long and 140 mm wide cylindrical tube of all stainless steel construction with covers at top and bottom. Total internal volume is 2.25 liters. Approximately 3/5 of this volume is filled with adsorbent while the rest is left as vapor gap. Within the bed, 8 identical rectangular fins are used in order to enhance heat transfer rate from oven outside to adsorbent inside. Each of those fins are 150 mm long, 65 mm wide and 5 mm thick. They are distributed with equal angles inside the bed with half of them are welded to outer shell and the other half are welded to the bottom cover. A single fin contains twelve T-type thermocouples on it in order to measure the temperature gradients on the adsorbent. They are organized in four rows and three columns at 24, 46 and 68 mm radii from the center of the bed and

17, 57, 97, and 135 mm longitudinally from the bottom of the canister. A spring loaded compression disk was used to compress the adsorbent to lower thermal contact resistances and seperate it from the vapor gap. For the vapor to better penetrate into adsorbent, eight mass transfer tubes are used between fins, sweeping from vapor gap to bottom. Each of them is 167 mm long and 10 mm wide. Those longitudinal tubes contain many 3 mm holes in order to allow vapor to be transported to adsorbent near to tubes. Tubes themselves are wrapped with a fine mesh for adsorbent not to flood into those tubes. Thus, vapor sweeping inside those tubes is able to penetrate deeper into the adsorbent both longitudinally and laterally. This bed is put inside a digital temperature regulated oven for controlling the adsorbent's temperature inside.

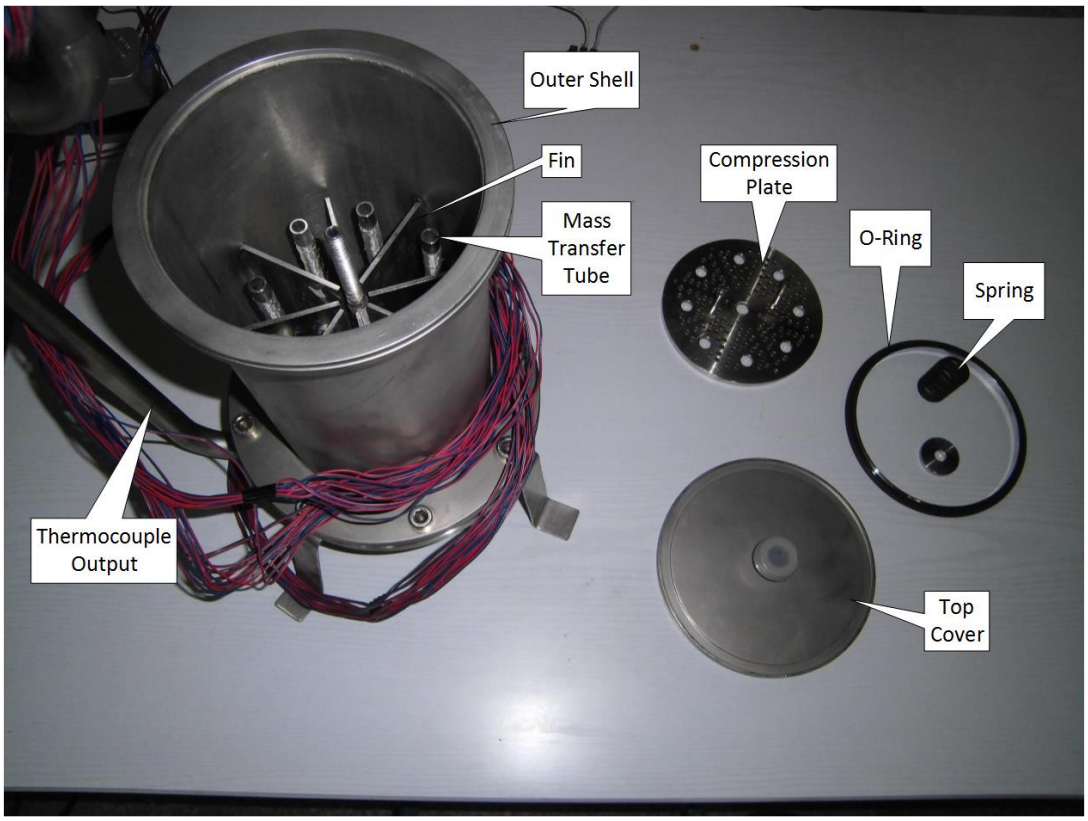

Figure 2.3: A photograph of stainless steel adsorbent bed and its components.

2.1.2 Evaporator/Condenser

Evaporator/Condenser is a 300 mm long and 50mm wide glass tube with stainless steel covers at top and bottom, all epoxy glued from outside in order to avoid gases that might disperse within evaporator/condenser. Inner diameter of the tube is 40

mm. Those covers are further clamped by bolts and nuts running through four equally spaced drilled holes on them. Two T-type thermocouples are used within the evaporator/condenser, each of them is held horizontally by a central stainless steel stick. All fastenings are done mechanically inside in order to avoid gas generation due to chemicals. Thermocouples are used to measure vapor and liquid temperatures, respectively. The thermocouple used to measure vapor-air temperature is located at approximately 30 mm below the upper steel cover, whereas the one used to measure liquid temperature is located at approximately 30 mm above the lower steel cover. Upper steel cover has a small 16 mm inner diameter pipe section drilled and welded to its center which allows it to be connected to rest of the system. Whole evaporator/-condenser is submersed within a temperature regulated water bath. Water level can be read on the transparent vertical milimeter scale on the glass. Thus, adsorption and desorption capacities can be calculated from difference of water levels.

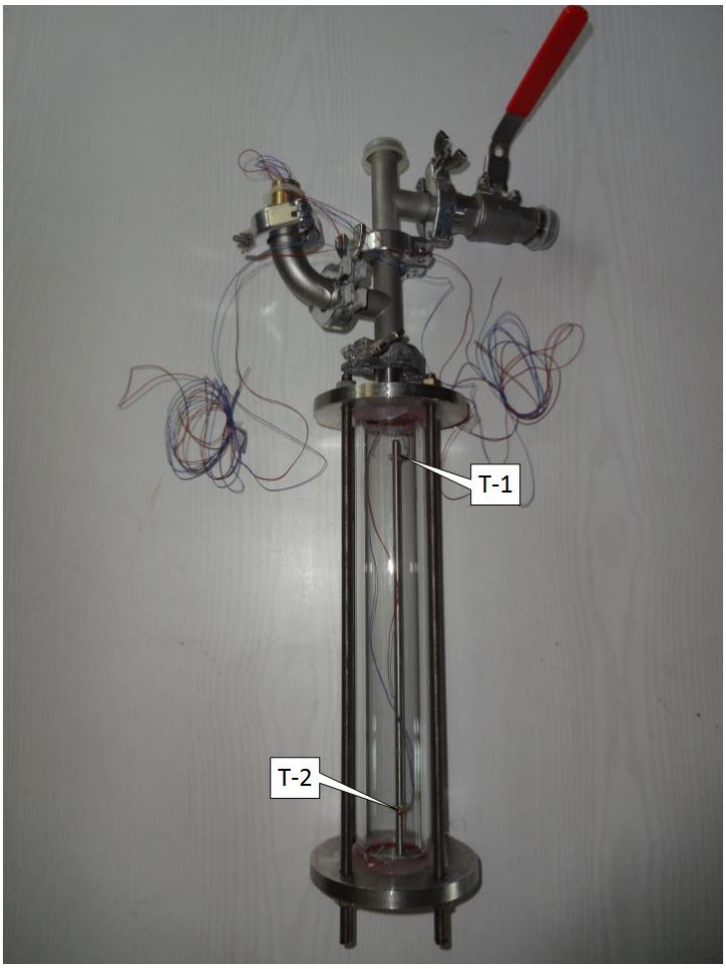

Figure 2.4: A photograph of evaporator/condenser (T-1 Top Thermocouple (Vapor); T-2 Bottom Thermocouple (Liquid)).

2.1.3 Oven and Water Bath

Oven is used to regulate the temperature of adsorbent bed inside it. It is an electrically heated, digitally temperature controlled oven with an air fan inside for providing enhanced heat transfer rates. Water bath is used to control the temperature of evaporator/condenser. It contains an evaporator coil of a conventional vapor-compression refrigerator and three 1.5kW electrical heaters for temperature regulation and a water pump for creating turbulence and water circulation inside for a uniform temperature distribution.

2.1.4 Pipings

A piping system containing valves, gaskets and feedthroughs connects adsorbent bed to evaporator/condenser. Inner diameter of the pipes are 16 mm. Filmwise condensation occurs when temperature on a surface is below than that of evaporator/condenser. In order to avoid filmwise condensation on pipeline, electrical flexible heaters were wrapped on and heated to a higher temperature. Temperature is controlled by a single thermocouple between pipe and heater which is held around 60°C. A two-stage Edwards RV-3 rotary vane vacuum pump is used to evacuate the whole system out of air and residual vapor. Total length of pipeline between valves V-1, V-2, V-4 and V-6 is around 2.13 meters. This particular part of pipeline was used as a constant volume to fill air in controlled amounts during experiments. By adjusting air pressure by fine valve within this constant volume, pre-determined amounts of air were injected to the apparatus for testing the effects of different amounts of air on adsorption.

2.1.5 Data Acquisition and Control

Datataker DT800 is used to store and read temperature and pressure datas as well as digitally controlling water bath and piping temperatures. The software DeLogger is used to control the datataker. Datataker is connected via COMM cable to computer. Temperatures of adsorbent bed, evaporator/condenser, water bath and pipeline are measured through T-type thermocouples. Pressures values are logged with a Kurt J. Lesker Series 910 Piezo/Pirani Transducer for Zeolite 13X and silica gel. Gas-independent piezo part of the transducer is used within the range of our experiments. An Edwards ASG1000 is used to read bed side pressure. For natural zeolite, an Omega PXM319 350 mbar range is used for logging values and an Omega PXM219 1 bar range is used to read bed side pressure. Specifications of data logging pressure transducers can be seen in Table 2.1 and Table 2.2. Datas are taken at each second for 25°C difference tests of Zeolite 13X. Rest of the datas are logged at each fifth second.

Table 2.1: Specifications of Kurt J. Lesker Series 910 Piezo/Pirani transducer.

Measuring range Pirani	$1x10^{-5}$ to 900 Torr
Measuring range Piezo	0.1 to 1500 Torr
Measuring range Combination	$1x10^{-5}$ to 1500 Torr
Accuracy Combination	1%: Range 10 to 1000 Torr
	10%: Range 10^{-4} to 10 Torr
Repeatability of Combination	1%: Range 10^{-2} to 1000 Torr
	5%: Range 10^{-3} to 1000 Torr
	10%: Range 10^{-4} to 1000 Torr
Setpoint Range Combination	$1x10^{-4}$ to 1500 Torr
Operating temperature	0 to 40°C
Bakeout temperature	85°C

Table 2.2: Specifications of Omega PXM319 350 mbar range transducer.

Static Accuracy	$\mp$0.25% FS BSL at 25°C; includes linearity, hysteresis and repeatability
Operating Temperature	-40 to 85°C
Compensated Temperature	0 to 50°C
Total Error Band	$\mp$1.5%

2.2 MATERIALS

Three adsorbents were tested in experiments. Namely, natural zeolite, silica gel and Zeolite 13X. Each one of them has unique working temperatures, adsorption capacities and porosities. Properties and details of those adsorbents are given below. As adsorbate, only de-ionized water is used with all three adsorbents. Therefore working pairs used in the experiment are:

- Natural zeolite-Water

- Silica gel-Water
- Zeolite 13X-Water

Above pairs are highly popular and highly available adsorptive pairs. They are widely used in adsorption refrigerators and solar cooling applications. Seemingly, there exist no research paper dedicated to investigate the effects of air on the adsorption properties of these materials. Therefore those three pairs were selected to be tested in this experiment.

2.2.1 Natural Zeolite

Natural zeolite used in the experiments is mined in Turkey by ROTA mining company. It is made of 88-95% klinoptilolit with about 0.5 mm grain size. Thermophysical properties are listed below:

Table 2.3: Thermophysical properties of natural zeolite [23, 43].

Appearance	Ivory white
Porosity	0.45-0.5
Average pore diameter (A)	4
pH	7-8
Bulk density (kg/m^3)	650-850
Melting temperature (°C)	1300
Mesopore surface area (m^2/gr)	29
Micropore surface area (m^2/gr)	11
Thermal conductivity (W/mK)	0.155

2.2.2 Silica Gel

White silica gel is used as adsorbent during silica gel experiments. White silica gel is a highly fine pore white semi-transparent glasslike hard mass in the forms of granules or spheres of various sizes. It has the characteristic of high adsorption under low relative humidity and can be used especially as desiccant, moisture-proof, rust inhibitor

as well as carrier of catalysis. Because of its extreme adsorption capacity white silica gel can be used for various applications such as dynamic adsorption which involves in the removal of water from a continuously flowing gas or liquid system or static adsorbtion which is the removal of moisture from spaces without induced air flow. White silica gel can be easily reactivated without a significant decrease for the adsorption efficiency of the product. Below are various properties of the silica gel that is used in the experiments:

Table 2.4: Chemical and physical specifications of silica gel.

Chemical formula	SiO_2 . n(H_2O) – amorphous form of silica
SiO_2 content	~ 99.7% (min 99.5%)
Humidity content	< 1.0%
Loss on ignition (650°C)	max. 6.5 %
Bulk density (g/l)	720
Mechanical strength	96%
Granular diameter	1 – 3 mm
Qualified ratio of granules	$\geq$ 90 %
pH (10% solution)	4 – 6

Table 2.5: Thermal specifications of silica gel.

Water vapor adsorption capacity at 25°C	20% relative humidity - 12% min.
	40% relative humidity - 24% min.
	80% relative humidity - 35% min.
Reactivation (regeneration) temperature	Max. 200°C

2.2.3 Zeolite 13X

Zeolite 13X is also known as 'Molecular Sieve type 13X'. It is a manufactured version of natural zeolite, and shares many performance features with it. Zeolite 13X typically has a higher adsorption capacity than the natural one. Working temperatures are similar in both. Molecular Sieve ZEOCHEM® Z10-01 is used in experiments.

ZEOCHEM® Z10-01 is the general purpose 13X grade. It is an alkali alumino-

silicate. It is the sodium form of the type "X" and has an effective pore opening of about 9 Angstrom (0.9 nm). This type has a wide range of applications in both liquid phase and gas phase where more polar molecules, such as moisture, carbon dioxide, hydrogen sulphide, mercaptans and other organics are selectively adsorbed on the basis of polarity. Typical applications include:

- Concurrent removal of carbon dioxide and moisture from air and other gases.
- The removal of hydrogen sulphide and mercaptans from hydrogen and hydrocarbon streams.
- Catalyst protection, removal of oxygenates from hydrocarbons.
- Removal of organic nitrogen compounds from hydrocarbon streams.

Below are some of the properties of ZEOCHEM® Z10-01:

Table 2.6: Thermophysical properties of Zeolite 13X.

Tapped bulk density (kg/m^3)	650
Bead size nominal (mm)	1.6-2.6
Crush strength (N)	20
Equilibrium water adsorption capacity (at 20°C, 50% relative humidity, 24 hours) (wt%)	26
Residual water content (550°C as shipped) (%)	1.5
Heat of adsorption (max.) (kJ/kg water)	4400
Specific heat (approx.) (kJ/kg°C)	1.07

2.3 EXPERIMENTAL PROCEDURES

Purpose of this experiment is to measure the effects of systematically put amounts of air to adsorption and desorption performance. In order to achieve this, two residual air amounts were determined to be injected along with a no-air case as this approach will reveal exponential trend on adsorption properties. Air was filled within the portion of pipeline by the fine valve between the closed valves V-1 to V-2, V-4 and V-7,

which have 2.13 m length and 16 mm diameter. Experiments were done with certain pressure values created within that volume. Amounts that were investigated are 0, 50 and 100 mbar pressures, respectively. 0, 25, 50 mbar pressures were used for tests with smaller adsorbent temperature difference on Zeolite 13X. As we have a nearly constant pipeline temperature or at least its gradients and a constant pipeline volume (2.13 m length × 16 mm diameter), we have a linearly increasing mass of air through linearly increasing pressure. Therefore, this experiment investigates how adsorption properties change with a linear increase of air mass in practice.

Two temperature values were determined to act as adsorption and desorption temperatures. The lower one being adsorption temperature and the higher one being desorption. Increase and decrease of temperatures between these values were done while valve V-1 was closed. After this process was complete, adsorption and desorption processes were started by opening that valve. This sudden start of sorption processes allows to compare adsorption and desorption kinetics between different amounts of residual air beyond that of final adsorption or desorption capacities. Maximum available temperature of the gaskets within adsorbent bed were rated at 200°C. Therefore, desorption temperature for high temperature working zeolites was selected as 160°C.

Natural zeolite was tested between working temperatures of 160°C-40°C. Each adsorption and desorption cycle between those temperatures were done on evaporator/-condenser temperatures of 10°C and 20°C. Adsorption and desorption performances were tested at 0, 50 and 100 mbar air pressures attained within the aforementioned volume for each sorption cycle on each evaporator/condenser temperature. Silica gel was tested similarly, albeit at working temperatures between 90°C-30°C, as silica gel has a higher adsorption capacity and work at lower temperatures more efficiently. Zeolite 13X was tested accordingly with the same working conditions of that of natural zeolite with the exception of 20°C evaporator/condenser temperature. Only 10°C evaporator/condenser temperature was used for full cycles between 160°C-40°C. However, additional experiments were done with this adsorbent. 90°C-65°C working temperatures were used with 20°C evaporator/condenser temperature and 140°C-115°C working temperatures were used with 10°C, 20°C and 30°C evaporator/condenser temperatures, respectively; each in turn were tested with 0, 25 and 50 mbar air pressures. This allowed to compare the effects of air on different ad-

sorbent temperature regimes and the exponential trend of air's effects with changing evaporator/condenser temperature.

Above descriptions of experimental variables are defined more concisely in Table 2.7.

Table 2.7: Experimental variables.

	Adsorbent working temperatures	Evaporator-condenser temperatures	Residual air pressures (within 2.13 m length × 16 mm diameter pipeline)
Natural Zeolite	160°C-40°C	10°C, 20°C	0 mbar, 50 mbar, 100 mbar
Silica Gel	90°C-30°C	10°C, 20°C	0 mbar, 50 mbar, 100 mbar
Zeolite 13X	160°C-40°C	10°C	0 mbar, 50 mbar, 100 mbar
	140°C-115°C	10°C, 20°C, 30°C	0 mbar, 25 mbar, 50 mbar
	90°C-65°C	20°C	0 mbar, 25 mbar, 50 mbar

2.3.1 Preliminary Procedures

Before the experiment, natural zeolite underwent through few procedures. It was first sifted through a micro-size screen in order to remove fine, dust-like particles. After that, it was washed using de-ionized water. It was than dried for 24 hours by spreading on a clean surface before being put in adsorbent bed.

Before being sealed into the bed, all three adsorbents were first heated in oven at their reported regeneration temperatures. A maximum temperature of 200°C is reported for silica gel and 240-300°C regeneration temperature for Zeolites 13X. Natural zeolite was reported to regenerate at 200°C [23]. Zeolite 13X, silica gel and natural zeolite were heated at 250°C, 175°C and 200°C, respectively. They were loosely distributed on a micro-size screen within oven during heating process. Mass of the adsorbents were constantly checked during this process. When the difference between two adjacent measurements were 1 grams, heating process was terminated. The last

measurement was taken as the dry mass of the adsorbent. This measurement would be used to determine the adsorption capacity values. The adsorbent that was going to be used for experiment was then sealed into adsorbent bed. Sealed bed was connected to rest of the apparatus for experimentation.

De-ionized water was fed to the evaporator/condenser via valve V-5. Water was fed whenever the water level fell significantly within evaporator/condenser. Valve V-5 was closed at all times except this procedure. Initial evacuation of air was done seperately at left and right side of valve V-3. After starting the vacuum pump, left side of valve V-3 was evacuated by opening valves V-2 and V-1 while V-3 was closed. Evacuation process was terminated once pressure gage I-1 reported a stabilized pressure below 3 mbar. Both oven and pipe heaters were held at higher temperatures during this process for vacuum drying of residual water, alcohol used for cleaning the equipment and gas created by vacuum grease within pipeline and bed. After the evacuation of bed side, valve V-1 was closed and valve V-4 was opened. Evaporator/condenser was evacuated while holding the water bath temperature constant. When the measured pressure at I-2 and the saturation pressure corresponding to liquid water temperature were approximately equal, evaporator/condenser was assumed to be evacuated and valve V-4 was closed. Remaining vapor and air was evacuated from the pipeline between valves V-1 and V-7 until pressure indicators reported a stabilized pressure below 3 mbar. Finally, valve V-2 and vacuum pump was closed. Similar evacuation processes were done after every experiment involving an adsorption and desorption cycle for each residual air pressure value, of each evaporator/condenser temperature; as each of the experiments involve inclusion of air.

As experimental apparatus contains many gaskets and feedthroughs, one of the most important procedure before experiment was to check if the apparatus was leaking air. Long observations of pressure were needed since each full scale adsorption-desorption experiment required two days to nearly a week until new vacuuming process. By closing valves V-2, V-3 and V-6 and opening V-1 and V-4, both pressure gages were observed for approximately 24 hours. Water bath was held at a constant temperature. Hence, constant saturation pressure. By closing valve V-3, the side that is leaking can be determined. If pressure on both sides were seen stabilized on a constant pressure below 3 mbar, it was assumed that no to minimal leakage occurs

and the experiments were started for that adsorbent. This leakage control procedure was done after each adsorbent was sealed into the bed and connected to rest of the apparatus for experimentation.

Finally, adsorbent temperature was stabilized at the respective desorption temperature and water bath was maintained at the first experiment's evaporator/condenser temperature; almost always the lowest one. All valves connecting bed to evaporator/-condenser was opened. This was done in order to let the system to reach equilibrium at the respective desorption temperature. Note that all adsorbents within the bed were heated at a temperature higher than their pre-determined desorption temperatures in order to measure their dry mass. Process was ended by closing valves V-1 and V-4 when both vapor and adsorbent reached an equilibrium.

2.3.2 Experimental Procedures

Initial evacuation within bed and pipes involved only air and other residual gases. First experiments required only the evacuation processes mentioned in the above section. However, after each experiment (which ends with desorption stage) significant amount of vapor had failed to condense within evaporator/condenser. Therefore a higher pressure was observed within the system than the saturation pressure of evaporator/condenser. Apart from that, filmwise condensation had occured inside pipelines during desorption as they were heated at a lower temperature (60°C) than desorption temperatures (160°C for zeolites, 90°C for silica gel). Thus, two different evacuation procedures were done for pipelines and bed after each experiment. Adsorbent bed was vacuumed first. Valve V-3 was closed while V-1 was left open. V-2 was opened and vacuum pump was started. Vacuuming process was continued until bed side pressure reached to the saturation pressure of the current experiment's water bath temperature (i.e. if the experiment would be done with 10°C water bath temperature, bed side would be equal to saturation pressure at 10°C) at the desorption temperature. Purpose of this procedure is to let the system reach equilibrium at the desorption temperature and current experiment's water bath temperature. Note that, there is no indicator of presence of air within the bed. Air was assumed to be evacuated after this process as attraction of water by adsorbent will act as a mass transfer resistance

of vapor to vacuum pump. Duration for bed side to reach equilibrium might last for a few hours depending on the amount of vapor within. During such a long process, non-adsorbable air was assumed to be evacuated first. After bed side was equilibrated with vapor at saturation pressure of water bath temperature, at the respective desorption temperature of adsorbent, valve V-1 was closed .

Second part of evacuation process was to evacuate evaporator/condenser. This was done exactly the same with that of preliminary procedure. Valve V-3 and V-4 were opened and vacuumed while water bath temperature was held constant. This vacuuming process was continued until internal pressure was equalized to saturation pressure of liquid water temperature. Valve V-4 was closed at the end of the process.

Lastly, pipeline was evacuated. Valves V-1 and V-4 were closed while V-3 and V-6 were opened. Pipe heaters were elevated to a higher temperature, in order to vaporize more water that was condensed upon pipe surfaces. After those, valve V-2 was opened and vacuum pump was started. Evacuation was continued until pressure within those pipes stabilized below 3 mbar. Finally, valve V-2 was closed and vacuum pump was shut down.

Each experiment was to be conducted at a certain evaporator/condenser temperature with a certain amount of residual air and between certain adsorbent temperatures (i.e. at 10°C evaporator/condenser temperature, 50 mbar residual air pressure, between 160°C-40°C adsorbent temperatures). After being equilibrated at the higher desorption temperature with a constant water bath temperature, adsorbent temperature was reduced to its adsorption temperature while valve V-1 was closed. Adsorbent temperature was observed to be stabilized there. At 0 mbar cases, no air was let in and simply valve V-6 remained close at all times. However, for experiments which involve residual air, valve V-6 was opened and air was let in slowly by fine valve V-7 to fill the pipeline from closed valves of V-1 to V-2 and V-4. This particular part of pipeline has a constant volume at 2.13 m of length and 16 mm of diameter. By controlling the pressure inside by fine valve, mass of air inside can be adjusted accordingly. So the residual air pressure values that are mentioned in the results (25 mbar, 50 mbar, 100 mbar) are in fact partial pressure values created by air within this portion of pipe. Air was let in until pressure indicators showed a sum of residual pressure within pipeline

which is just below 3 mbar and the predetermined air pressure. So the final pressure read on pressure sensors when this process was over was equal to $P_{tot} = P_A + P_{res}$. After that, valves V-7 and V-6 were closed and V-1 was opened for more uniform distribution of air throughout the system. Few seconds later V-1 was closed as well. Finally, valve V-4 was opened and vapor was let to fill the pipeline. Indicated pressure was confirmed to be consistent with saturation pressure of evaporator. Lastly, adsorption process was started by opening valve V-1.

Equilibrium conditions for adsorption were defined as all temperatures within adsorbent were at least 5°C within the adsorption temperature and both vapor and liquid temperatures would be 1°C within water bath temperature. When equilibrium was reached, valves V-1 and V-4 were closed. For desorption stage, adsorbent temperature was raised to respective desorption temperature while valve V-1 was closed. After adsorbent temperature was observed to be stabilized at desorption temperature, desorption stage was started by opening valve V-1 while valve V-4 was open. Equilibrium in desorption stage was treated differently. As mentioned before, due to hysteresis effect, not all vapor condenses, therefore pressures higher than saturation pressure of water bath remain. Three indications were considered for equilibria. First was the stabilization of internal pressure, second was about average adsorbent temperature to reach within 5°C of desorption temperature, other was for vapor and liquid temperatures to be 1°C within water bath temperature. When these three indicators were observed, desorption stage was terminated by closing valves V-1 and V-4.

All of the above processes were repeated for each and every experiment.

2.3.3 Calculations

Calculations had to be done in order to find adsorption/desorption capacities from the raw data of water level differences. These calculations are shown below:

$$D = 40\,mm = 0.04\,m \qquad D_{stick} = 5\,mm = 0.005\,m \tag{2.1}$$

$$X_{ads} = X_{des} = \frac{|\Delta L| \cdot \rho_{water} \dfrac{\pi \left(D^2 - D_{stick}^2\right)}{4}}{m_{ads}} \tag{2.2}$$

2.3.4 Uncertainties

All error values given in datas represent only the reading errors. Error regarding the dry mass of adsorbent was due to gram scale of weight. For pressure sensor, reported error value in manual was taken into account. Qualitative errors may be present due to small amount of residual water or air in system before experiment, possible slight leakages during experiment, position of waterline within evaporator/condenser, film-wise condensation, slight differences in temperatures of oven and water bath and so on. These may also affect the repeatability and accuracy of the experiments. For this reason, adsorbent working temperatures and residual air ranges were taken as large as possible with the exception of small temperature difference experiments of Zeolite 13X. Thus, any qualitative errors occurred during experiment would not drastically change the general results of the experiments. Calculations of reading errors are presented below:

A millimeter scale was used on evaporator/condenser when measuring the differences in water level, which gives the amount of water adsorbed/desorbed by calculation. Calculation of reading error for adsorption and desorption capacities is presented below:

$$E = \frac{\mp 0.5\,mm \cdot 10^{-3} \rho_{water} \dfrac{\pi \left(D^2 - D_{stick}^2\right)}{4}}{m_{ads}} \tag{2.3}$$

Upper and lower reading errors concerning the ratio of desorption to adsorption capacity as percentage are calculated as below:

$$E_{d/a\,upper} = \left(\frac{X_{des} + E}{X_{ads} - E} - \frac{X_{des}}{X_{ads}} \right) 100\ \% \tag{2.4}$$

$$E_{d/a\,lower} = \left(\frac{X_{des} - E}{X_{ads} + E} - \frac{X_{des}}{X_{ads}} \right) 100\ \% \tag{2.5}$$

CHAPTER 3

RESULTS

The results are defined in two main parts for each adsorbent. First part is on the effects on equilibrium properties, which include tables and graphs of adsorption and desorption capacities and their ratios to each other as well as reductions from the 0 mbar, no-air case by percentage. Second degree polynomials were fitted to datas in the graphs in this section. Adsorption and desorption capacity is the mass amount of water adsorbed or desorbed normalized by the dry mass of adsorbent. Desorption capacity to adsorption capacity ratio is the ratio of these two. Although hypothetically the process is completely reversible, hysteresis effect was observed in all cases. Condensed water was always less than the evaporated water. Part of this fact is due to vapor condensing within the pipeline.

Second part is dedicated to transient effects on both adsorption and desorption. These sections contain graphs of change of gas pressure, gas temperature and average adsorbent temperature over time. Gas pressure datas were taken by the transducer I-2. Omega PXM319 was used for natural zeolite datas and Kurt J. Lesker Series 910 Piezo/Pirani Transducer was used for the rest. Gas temperature datas come from the upper thermocouple within the evaporator/condenser. Average adsorbent temperature datas were attained from the average temperature of twelve thermocouples inside the adsorbent bed. Datas were logged for around 20.5 hours due to datataker limitations. However, most experiments continued well beyond until they reached an equilibrium. Gas pressure and temperature are properties of vapor-air mixture and only vapor for no-air experiments.

Dry masses and partial air pressures within bed and pipeline between valves V-1, V-2,

V-4 and V-6 are given in Table 3.1 for each adsorbent.

Table 3.1: Dry masses and partial air pressures for different adsorbents.

	Natural Zeolite	Silica Gel	Zeolite 13X
Dry mass (kg)	1.542 ∓ 0.001	1.691 ∓ 0.001	1.380 ∓ 0.001
Air pressure created within bed and pipeline with 100 mbar air pressure only within pipeline (mbar)	7.1 ∓ 0.9	7.3 ∓ 0.9	9.0 ∓ 0.9

3.1 NATURAL ZEOLITE

For this adsorbent, most experiments were ended just after the datas for transient results were collected. Namely, around 20.5 hours after the experiment had started. As this adsorbent has the lowest adsorption capacity, reaching an equilibrium was fairly quick.

3.1.1 Effects on equilibrium properties

It can be easily seen in Table 3.2, Figure 3.1 and Figure 3.2 that adsorption capacity of 10°C evaporator temperature showed a sharper decrease with linear increase of air mass than that of 20°C. Not only 10°C was effected more, it showed a logarithmic decay of adsorption capacity whereas the decay of 20°C case was rather more linear. Reductions in adsorption capacity were significantly lower for 20°C case comparing to most other experiments. Decay characteristic of 10°C case was similar to that of Zeolite 13X for the same evaporator temperature.

Both condenser temperatures showed similar reduction values in desorption capacities at 50 mbar. However, reduction for 10°C case was greater than that of 20°C at 100 mbar air pressure; almost down to zero. Reduction in desorption capacities were always lower than those of silica gel but higher than that of Zeolite 13X. Finally, 20°C case showed an exponential decay, while decay of 10°C case was almost linear. Change of desorption capacities can be seen in Table 3.3, Figure 3.3 and Figure 3.4.

Desorption stage of natural zeolite showed less of the hysteresis effect than that of Zeolite 13X but more than the silica gel for no-air cases. Amount of desorbed water in condenser started around half of the adsorbed value for no-air cases. Thereafter, 10°C case fell linearly whereas 20°C case showed an exponential decay, much like the reduction of desorption capacities. Reduced ratio with increasing residual air effectively means that desorption stage was more affected by an increase in air pressure. Table 3.4 and Figure 3.5 show the amount of hysteresis over changing residual air pressures.

Table 3.2: Changes in adsorption capacities for natural zeolite, 10°C, 20°C evaporator temperatures, 160°C-40°C adsorbent working temperatures.

	10°C		20°C	
Residual air	X_{ads}	Reduction	X_{ads}	Reduction
0 mbar	0.0553 ∓ 0.0004		0.0573 ∓ 0.0004	
50 mbar	0.0473 ∓ 0.0004	14%	0.0529 ∓ 0.0004	8%
100 mbar	0.0100 ∓ 0.0004	82%	0.0468 ∓ 0.0004	18%

Table 3.3: Changes in desorption capacities for natural zeolite, 10°C, 20°C condenser temperatures, 160°C-40°C adsorbent working temperatures.

	10°C		20°C	
Residual air	X_{des}	Reduction	X_{des}	Reduction
0 mbar	0.0277 ∓ 0.0004		0.0256 ∓ 0.0004	
50 mbar	0.0120 ∓ 0.0004	57%	0.0124 ∓ 0.0004	52%
100 mbar	0.0004 ∓ 0.0004	99%	0.0060 ∓ 0.0004	77%

Table 3.4: Desorption capacity to adsorption capacity ratios for natural zeolite, 10°C, 20°C evaporator/condenser temperatures, 160°C-40°C adsorbent working temperatures.

Residual air	10°C	20°C
0 mbar	50%	45%
50 mbar	25%	23%
100 mbar	4%	13%

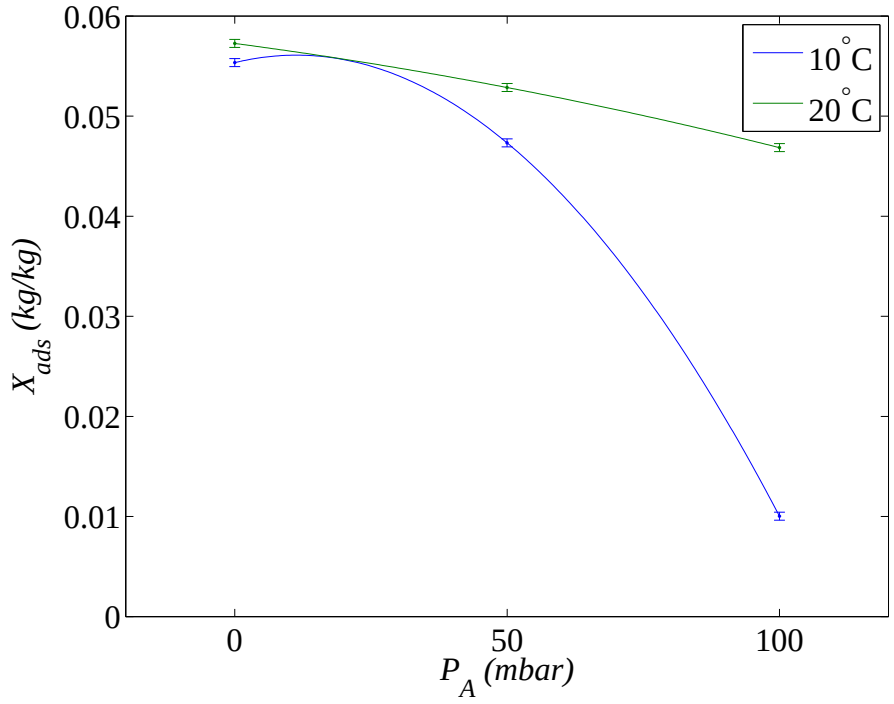

Figure 3.1: Adsorption capacity vs. Residual air pressure graph for natural zeolite, 10°C, 20°C evaporator temperatures, 160°C-40°C adsorbent working temperatures.

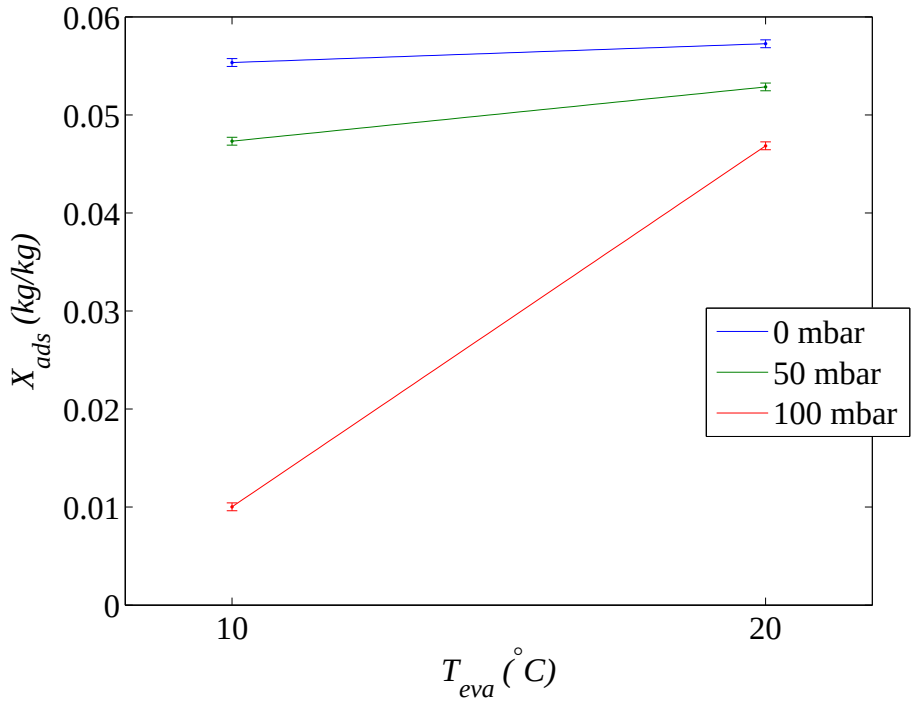

Figure 3.2: Adsorption capacity vs. Evaporator temperature graph for natural zeolite, 10°C, 20°C evaporator temperatures, 160°C-40°C adsorbent working temperatures.

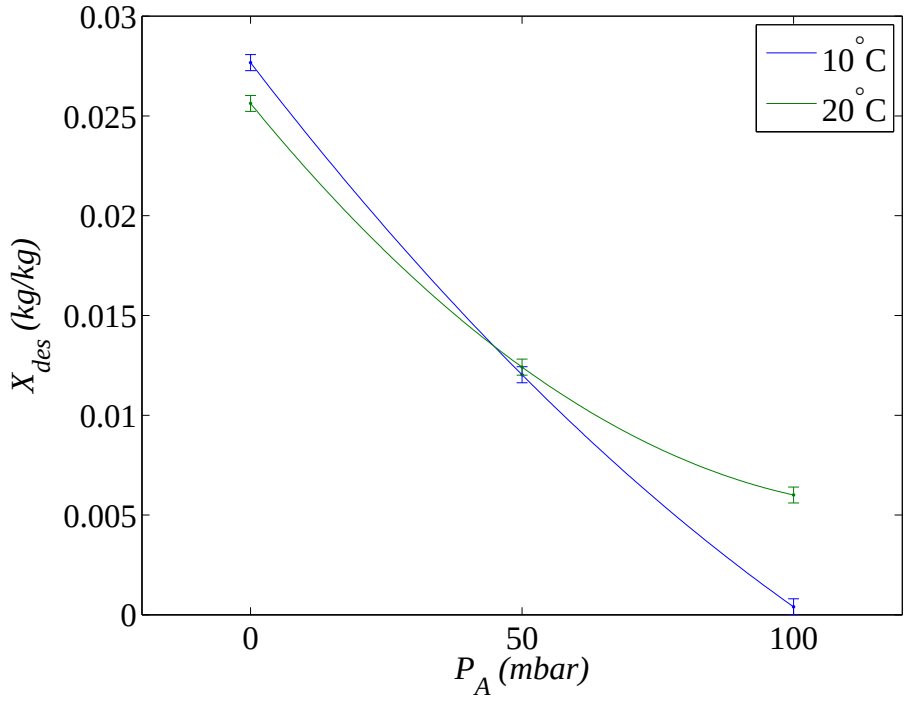

Figure 3.3: Desorption capacity vs. Residual air pressure graph for natural zeolite, 10°C, 20°C condenser temperatures, 160°C-40°C adsorbent working temperatures.

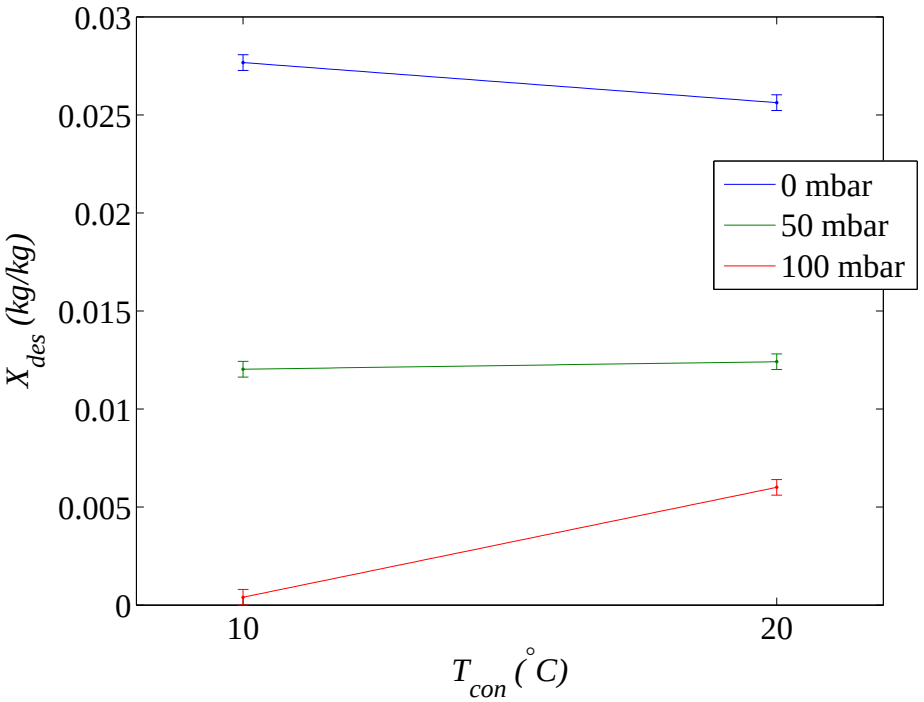

Figure 3.4: Desorption capacity vs. Condenser temperature graph for natural zeolite, 10°C, 20°C condenser temperatures, 160°C-40°C adsorbent working temperatures.

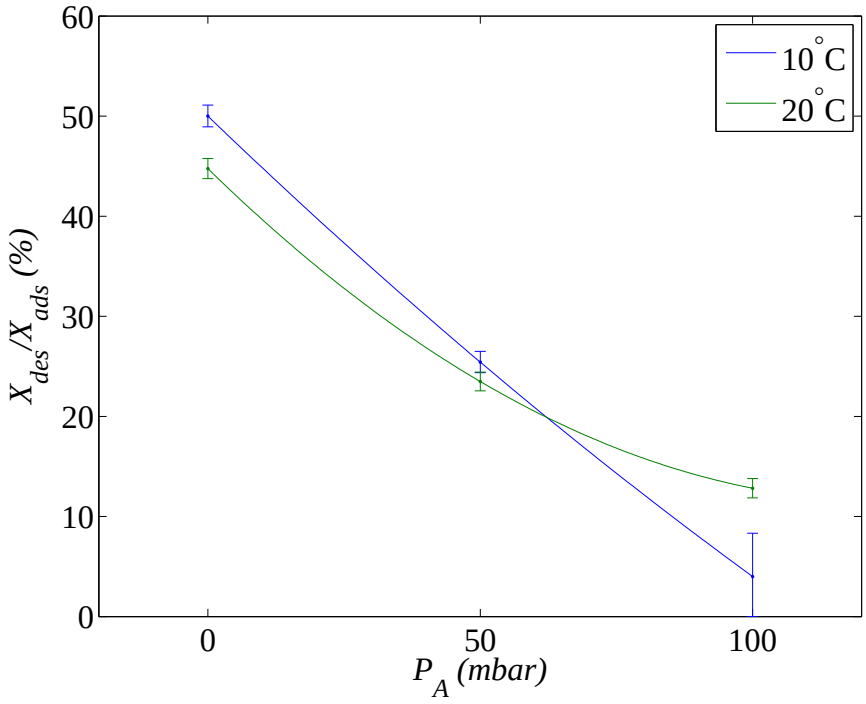

Figure 3.5: Ratio of desorption capacity to adsorption capacity vs. Residual air pressure graph for natural zeolite, 10°C, 20°C evaporator/condenser temperatures, 160°C-40°C adsorbent working temperatures.

3.1.2 Transient Effects on Adsorption

Changes in gas pressures are given in Figure 3.6 and Figure 3.7. For 10°C evaporator temperature and 100 mbar air pressure case, we can see gas pressure increasing linearly especially on the latter part of the experiment. This is not due to an air leakage as might be expected. The 10°C evaporator temperature with 100 mbar air pressure case for natural zeolite was the most extreme in a way that adsorption capacity was the lowest. It is also observable from the fact that reduction in pressure was not far from that of saturation pressure at the earlier part of the experiment. Thus, adsorption ended early. The reason for that increase in pressure was due to oven and pipe tapes heating the vapor within. As adsorption process ended, vapor lingers within the apparatus without being adsorbed and thus, heated up. Although more water was expected to be adsorbed due to higher pressure and temperature, thus giving an erroneously higher adsorption capacity value, this had not happened. There was no increase in corresponding gas temperature values, thus no water was adsorbed out of the evapo-

rator. Some of the vapor lingering within pipeline and canister might be adsorbed but that would only constitute a negligible amount.

Another fact to note is the relative retardation of gas pressure at 10°C, 0 mbar case. This is especially different from the 20°C case which have almost converging pressures for all air pressures for the latter part of the experiments. While part of this may be due to a larger adsorption capacity of no-air case, main reason is attributable to ice sheet occurred at the top of the surface of water, effectively stopping the water to evaporate. This can also be observed from the gas temperature graph in Figure 3.8 reaching nearly to -15°C; well below the freezing point for water. Gas pressure changes for 20°C were different. All different air pressure cases were characterized by an initial sharp decrease and then a sharp increase in pressure with lower minimas for lower air pressures and almost converging curves for the latter part of the experiment. This indicates more vapor was adsorbed at earlier stages of experiments.

Gas temperatures mostly followed suit. They showed similar characteristics to those of gas pressures. Only 10°C, 0 mbar case was different as it showed a highly erratic pattern as it reached to equilibrium. As mentioned before, this is due to the ice sheet occurred on top of the water line, stopping adsorption in process. Figure 3.8 and Figure 3.9 show the changes in gas temperatures.

As adsorbent adsorbs the water, it generates heat and increases the temperature of itself. Each graph in Figure 3.10 and Figure 3.11 shows a higher maximum temperature with lower air pressures as expected, with the exception of 10°C, 0 mbar case. It clearly shows the delaying effect of ice sheet with a longer but lower maximum temperature region. Note how maximas occur at similar moments albeit with different values. Except the aforementioned case, curves were smoother than other adsorbents. 20°C cases showed higher increase in temperatures as more water was adsorbed. Hence, higher heat.

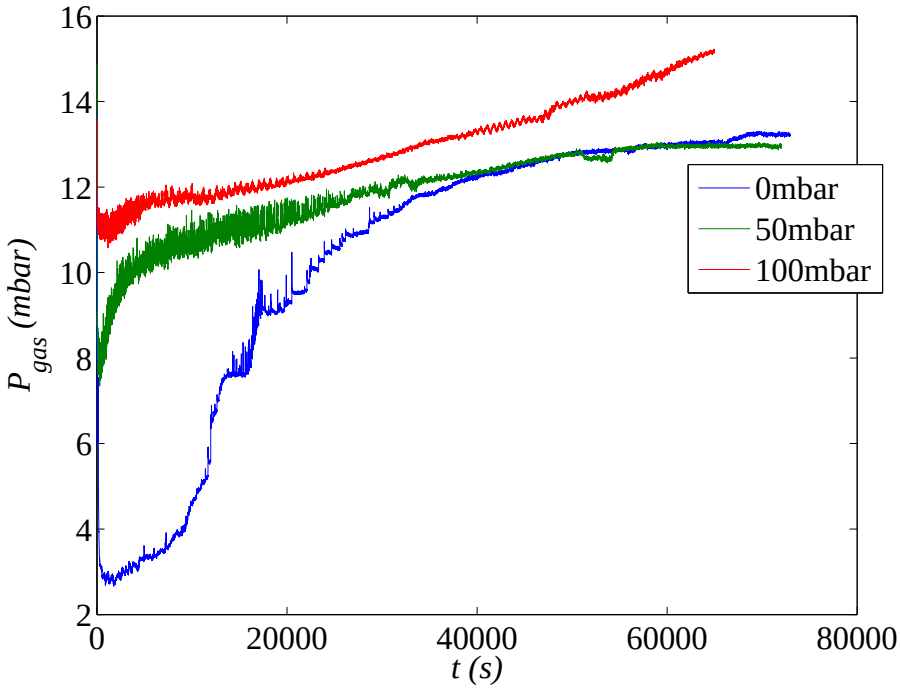

Figure 3.6: Gas pressure vs. Time graph of adsorption process for natural zeolite, 10°C evaporator temperature.

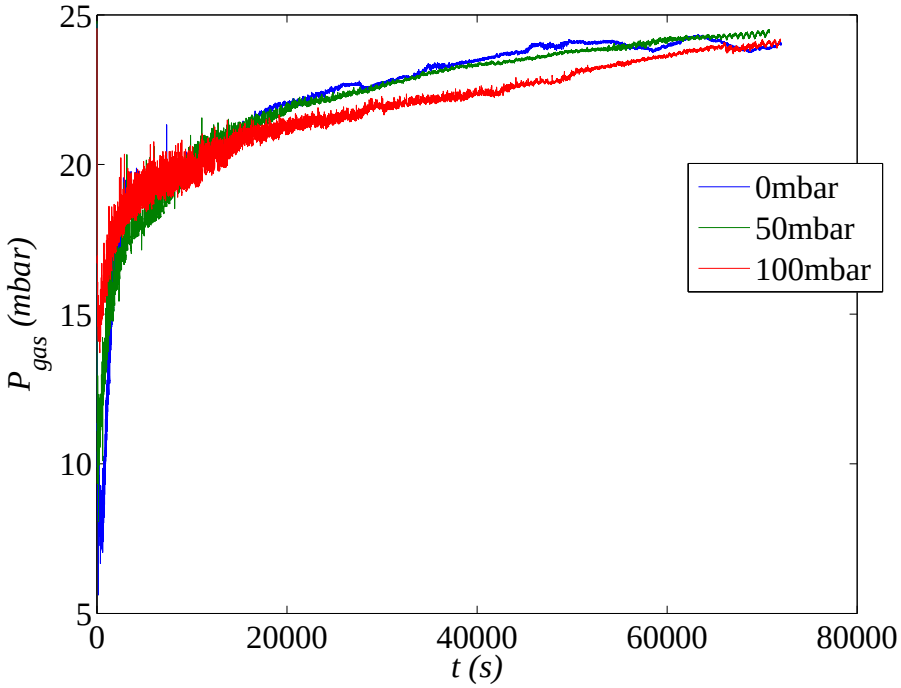

Figure 3.7: Gas pressure vs. Time graph of adsorption process for natural zeolite, 20°C evaporator temperature.

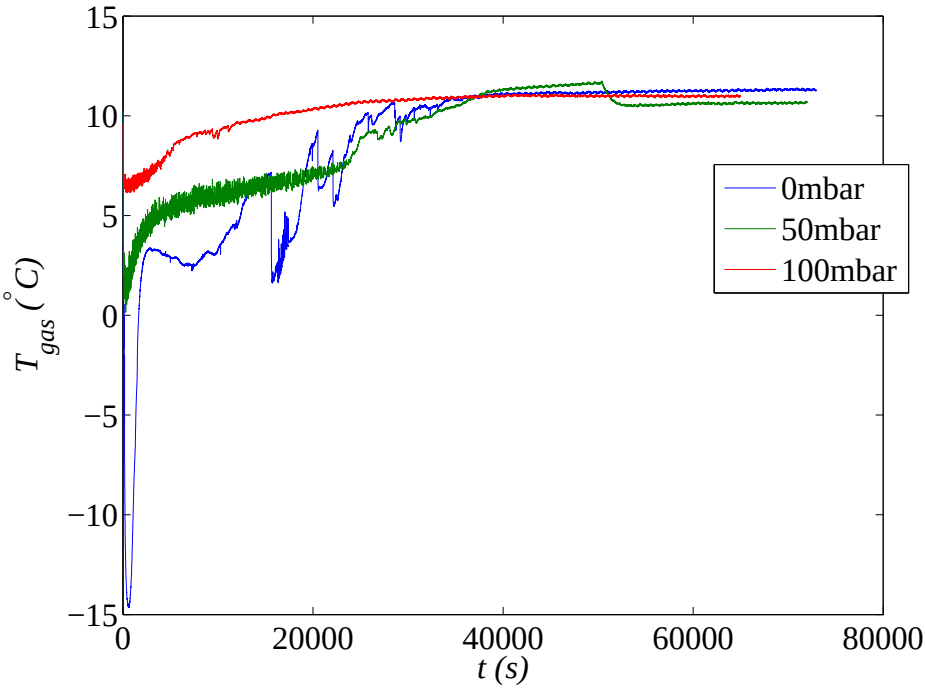

Figure 3.8: Gas temperature vs. Time graph of adsorption process for natural zeolite, 10°C evaporator temperature.

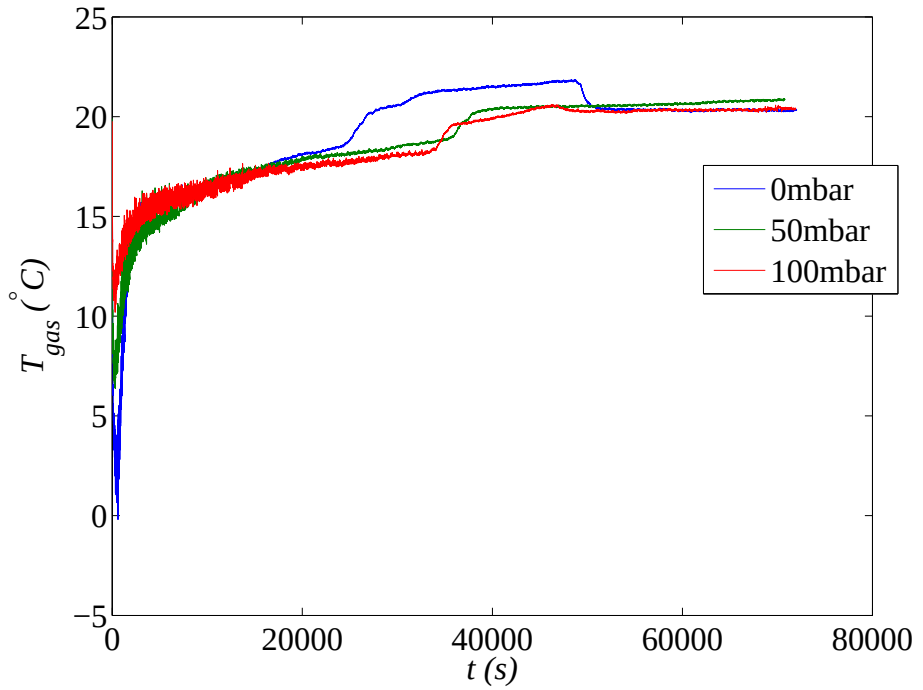

Figure 3.9: Gas temperature vs. Time graph of adsorption process for natural zeolite, 20°C evaporator temperature.

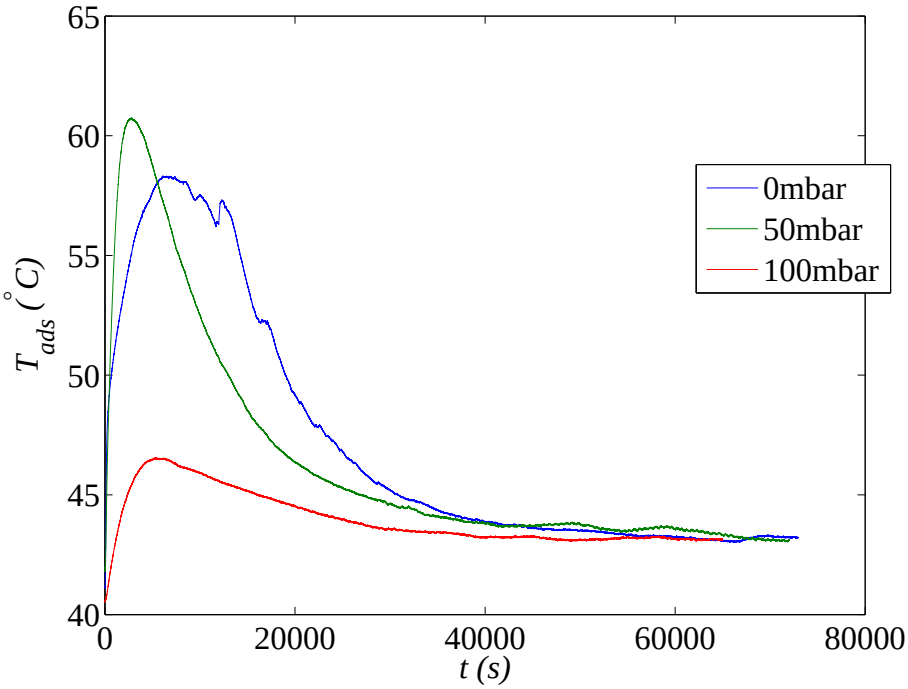

Figure 3.10: Average adsorbent temperature vs. Time graph of adsorption process for natural zeolite, 10°C evaporator temperature.

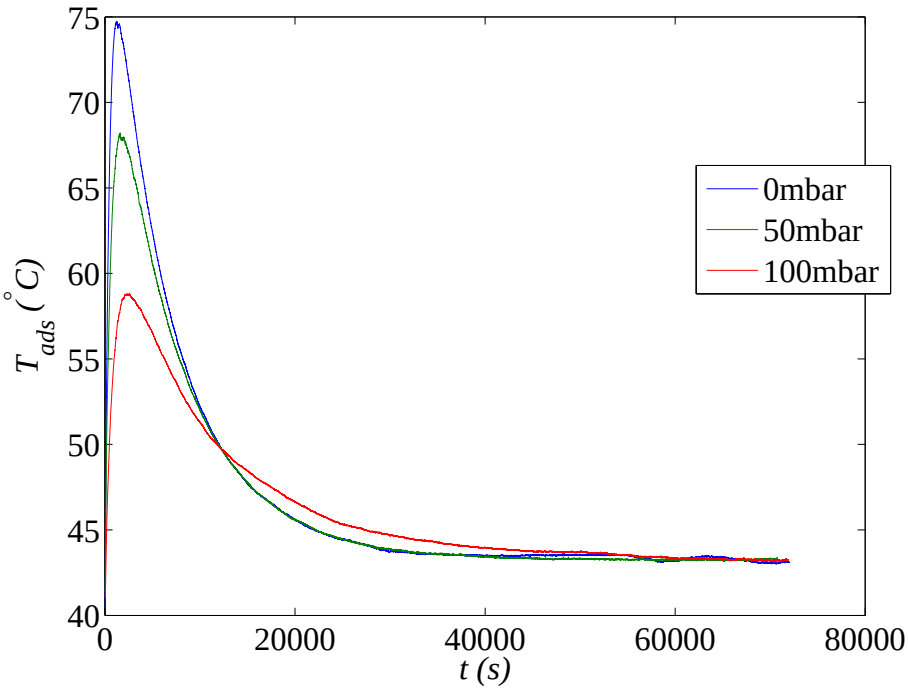

Figure 3.11: Average adsorbent temperature vs. Time graph of adsorption process for natural zeolite, 20°C evaporator temperature.

3.1.3 Transient Effects on Desorption

Gas pressures over time graphs in Figure 3.12 and Figure 3.13 showed initial decrease with almost constant pressure higher than the saturation pressure of condenser thereafter, implying much of the vapor failed to condense. Higher difference in gas pressures were observed for lower air pressures, as more vapor condensed in those cases. 10°C, 100 mbar case showed the smallest difference among all, immediately reaching a steady pressure as the adsorption capacity was the lowest desorbed vapor was also minimal. Note that pressure is seen to slowly increase in that case due to heat coming from oven and electrical tapes, similar to the adsorption case of the same experiment.

In Figure 3.14 and Figure 3.15 only first 7000 and 3000 seconds of gas temperature changes are shown, as they reached to equilibrium quickly for both of the experiments. That also means that most of the condensation within condenser occured within that time period. 20°C cases reached equilibrium more quickly than 10°C cases, almost half the time 10°C cases reached. Note that temperature of 10°C, 100 mbar case remains almost unchanged over time. Cases with lower air pressures reached water bath temperature later since condensed water was more.

Lower air pressures yielded lower temperatures through time in Figure 3.16 and Figure 3.17 as more water desorbed and expanded and cooled down the adsorbent, as expected. As the experiment with lowest condenser temperature and highest amount of residual air, 10°C, 100 mbar case showed almost unchanged temperature over time. This means only a small amount of vapor desorbed, as seen in its desorption capacity. Unlike other adsorbents, average adsorbent temperature changes for desorption did not show the constant temperature regimes of other experiments. All cases showed a steady increase to desorption temperature and reached it within the time frame of transient data logging range. This may indicate that there should be minimal undesorbed water when the experiment started, if any.

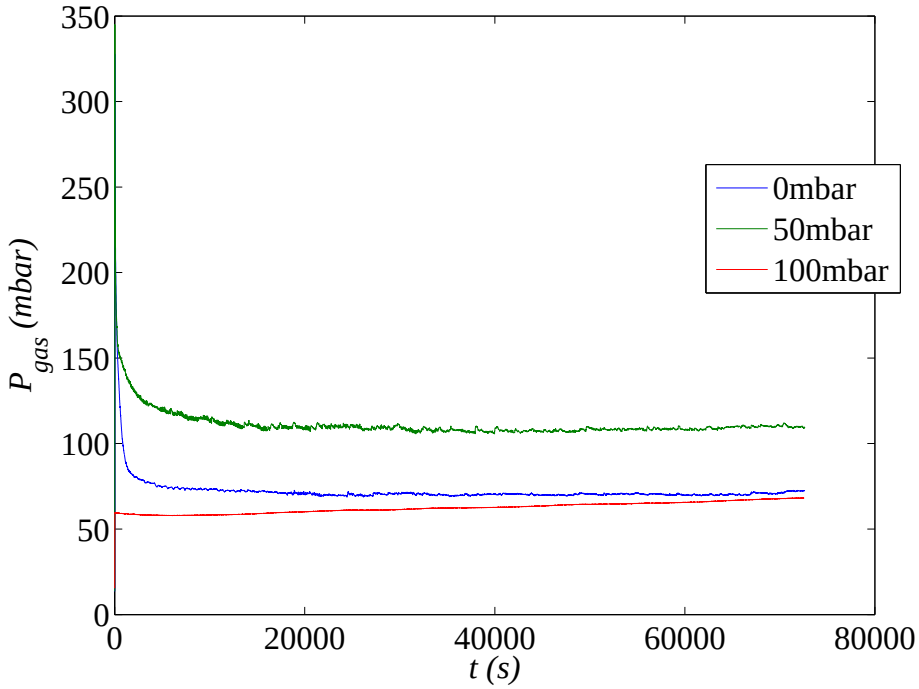

Figure 3.12: Gas pressure vs. Time graph of desorption process for natural zeolite, 10°C condenser temperature.

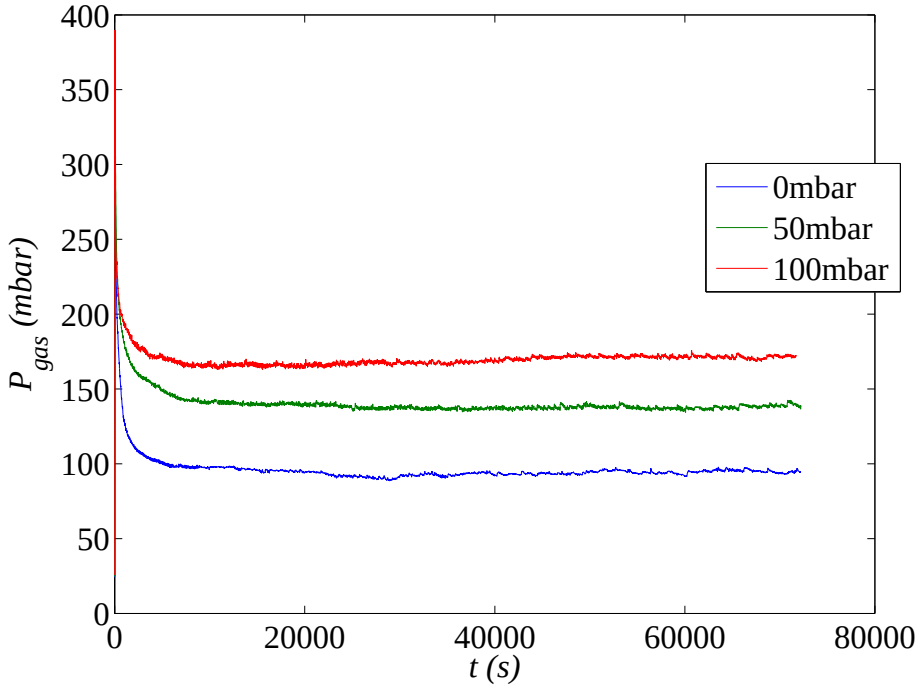

Figure 3.13: Gas pressure vs. Time graph of desorption process for natural zeolite, 20°C condenser temperature.

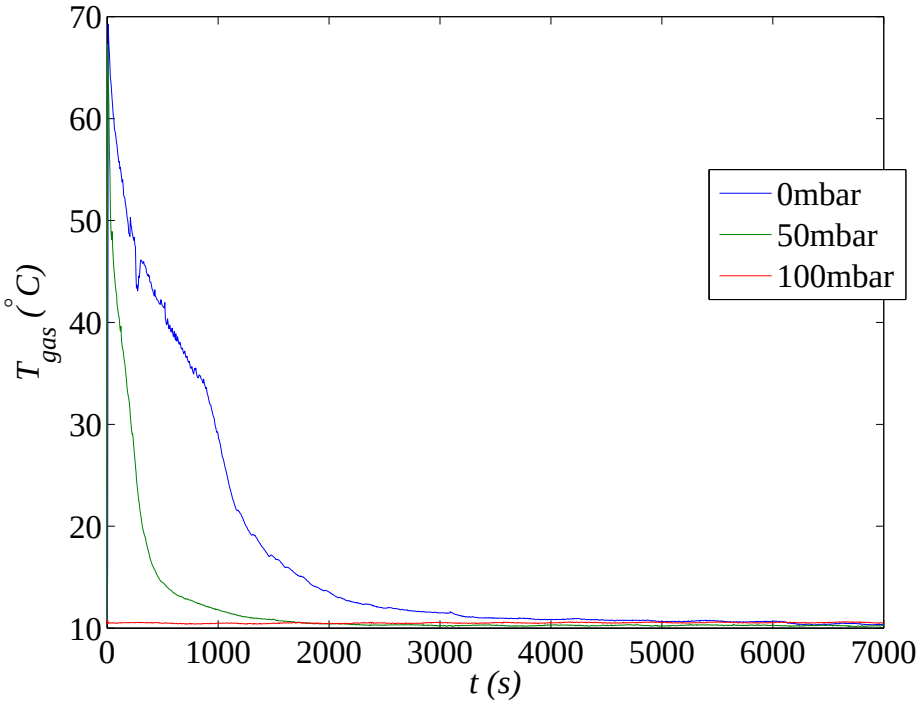

Figure 3.14: Gas temperature vs. Time graph of desorption process for natural zeolite, 10°C condenser temperature.

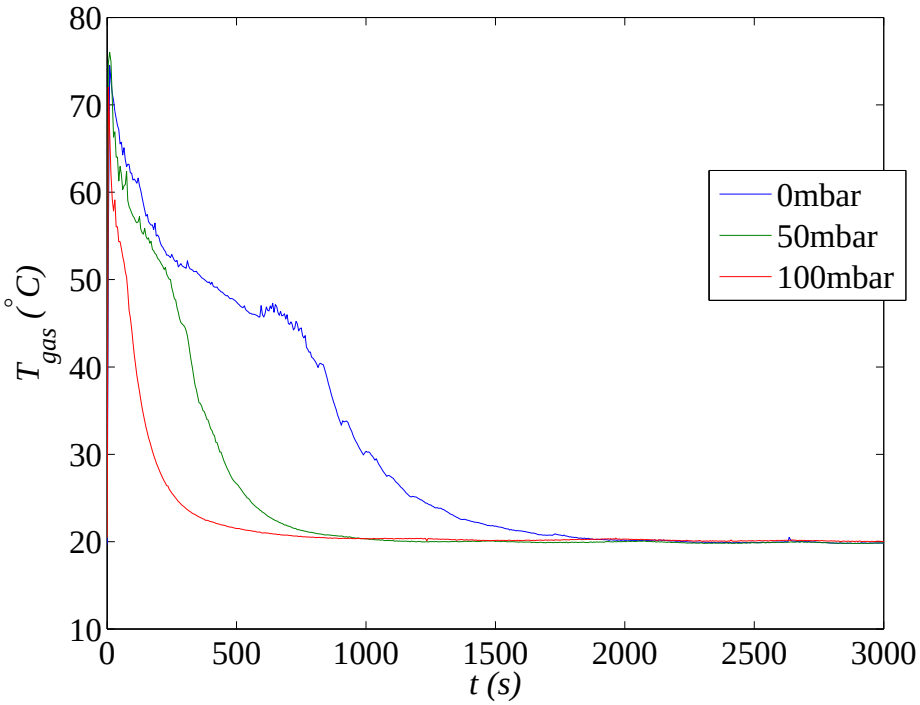

Figure 3.15: Gas temperature vs. Time graph of desorption process for natural zeolite, 20°C condenser temperature.

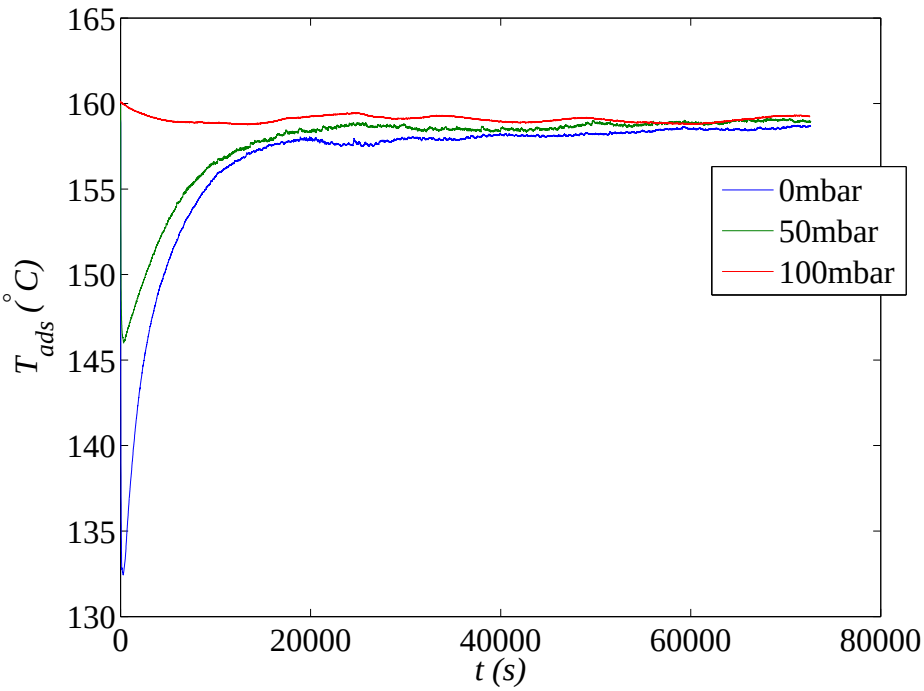

Figure 3.16: Average adsorbent temperature vs. Time graph of desorption process for natural zeolite, 10°C condenser temperature.

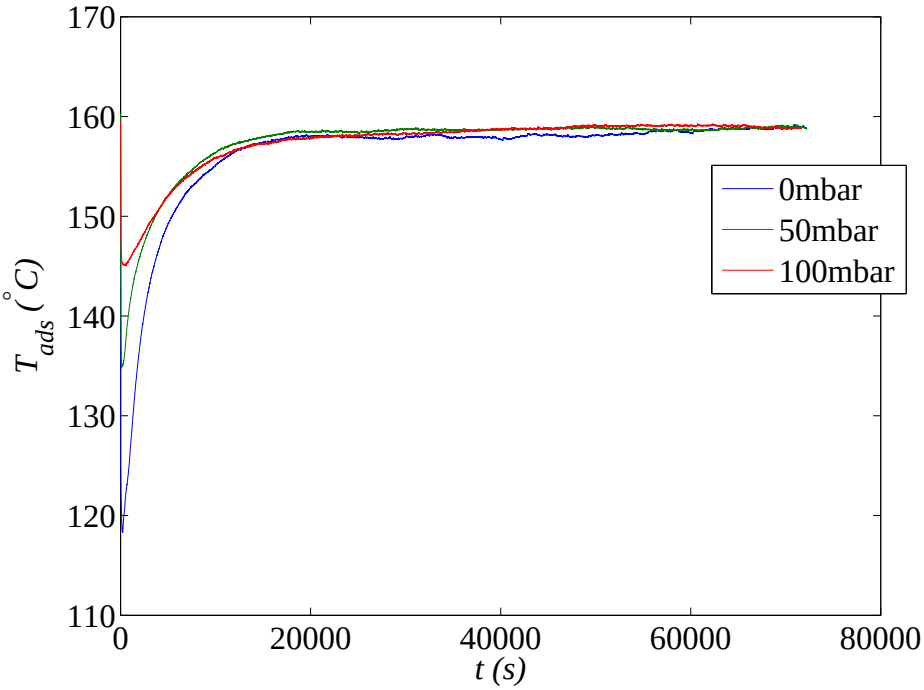

Figure 3.17: Average adsorbent temperature vs. Time graph of desorption process for natural zeolite, 20°C condenser temperature.

3.2 SILICA GEL

Among three, silica gel was the one with highest adsorption capacity even with its lower temperature difference between desorption and adsorption temperatures. It was also chemically different than the zeolites. Silica gel adsorbs more effectively at lower temperatures than zeolites. Therefore, working temperatures were lower. It was the most affected adsorbent with the presence of 50 mbar of residual air: adsorption and desorption capacities reduced more than any other. As this adsorbent had the highest adsorption capacity, reaching an equilibrium took longer than any other adsorbent and well beyond the time scale of around 20.5 hours where datas for transient cases gathered. Therefore, datas for transient cases should be considered with that information.

3.2.1 Effects on equilibrium properties

Changes in adsorption and desorption capacities by increasing air are given in Table 3.5, Figure 3.18, Figure 3.19 for adsorption and Table 3.6, Figure 3.20, Figure 3.21 for desorption. Larger reduction in both adsorption and desorption capacities was observed for lower 10°C evaporator/condenser temperature by percentage. This was also the case for desorption to adsorption ratio shown in Table 3.7 and Figure 3.22. Although both evaporator/condenser temperatures showed similar ratios at 0 mbar, 10°C case reduced further with an increase in residual air pressure. Note that for 20°C case, ratio of desorption to adsorption showed an almost linear decrease. As reduction in desorption/adsorption ratio was observed with increasing air pressure for both evaporator/condenser temperatures, we can say that desorption was affected more than adsorption with increasing air pressure. With the exception of desorption at 10°C temperature which already reduced to near zero at 50 mbar, both adsorption and desorption decay patterns were exponential. Especially, exponential decay of adsorption pattern was worthy of note, since logarithmic decay pattern was observed for all adsorption experiments for larger temperature load with zeolites. Adsorption capacity decay characteristics for both evaporator temperatures were similar.

Table 3.5: Changes in adsorption capacities for silica gel, 10°C, 20°C evaporator temperatures, 90°C-30°C adsorbent working temperatures.

	10°C		20°C	
Residual air	X_{ads}	Reduction	X_{ads}	Reduction
0 mbar	0.0943 ∓ 0.0004		0.1727 ∓ 0.0004	
50 mbar	0.0450 ∓ 0.0004	52%	0.1041 ∓ 0.0004	40%
100 mbar	0.0223 ∓ 0.0004	76%	0.0759 ∓ 0.0004	56%

Table 3.6: Changes in desorption capacities for silica gel, 10°C, 20°C condenser temperatures, 90°C-30°C adsorbent working temperatures.

	10°C		20°C	
Residual air	X_{des}	Reduction	X_{des}	Reduction
0 mbar	0.0695 ∓ 0.0004		0.1347 ∓ 0.0004	
50 mbar	0.0007 ∓ 0.0004	99%	0.0420 ∓ 0.0004	69%
100 mbar	0.0000 ∓ 0.0004	100%	0.0051 ∓ 0.0004	96%

Table 3.7: Desorption capacity to adsorption capacity ratios for silica gel, 10°C, 20°C evaporator/condenser temperatures, 90°C-30°C adsorbent working temperatures.

Residual air	10°C	20°C
0 mbar	74%	78%
50 mbar	2%	40%
100 mbar	0%	7%

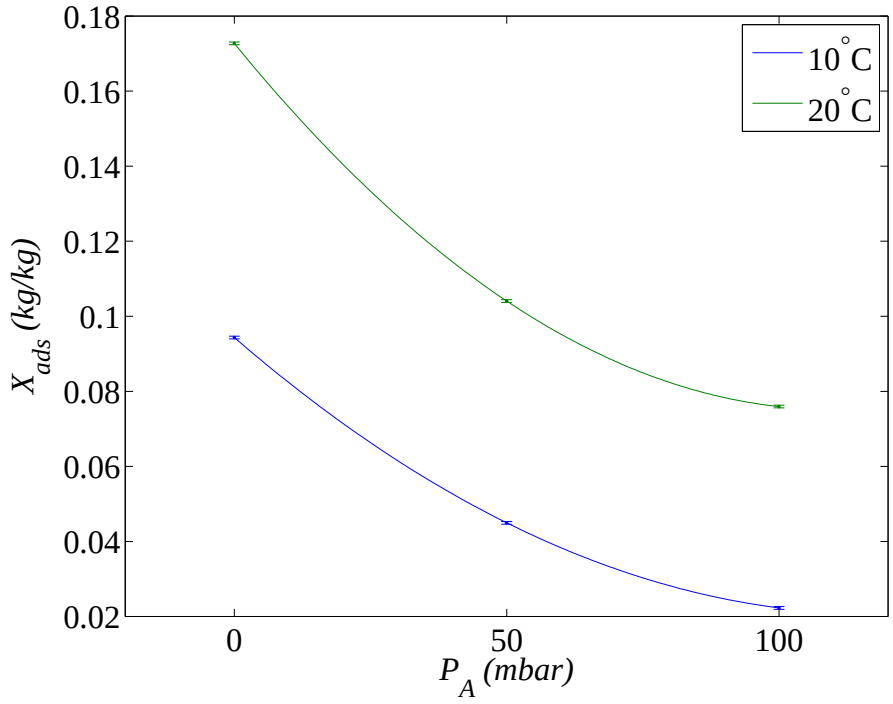

Figure 3.18: Adsorption capacity vs. Residual air pressure graph for silica gel, 10°C, 20°C evaporator temperatures, 90°C-30°C adsorbent working temperatures.

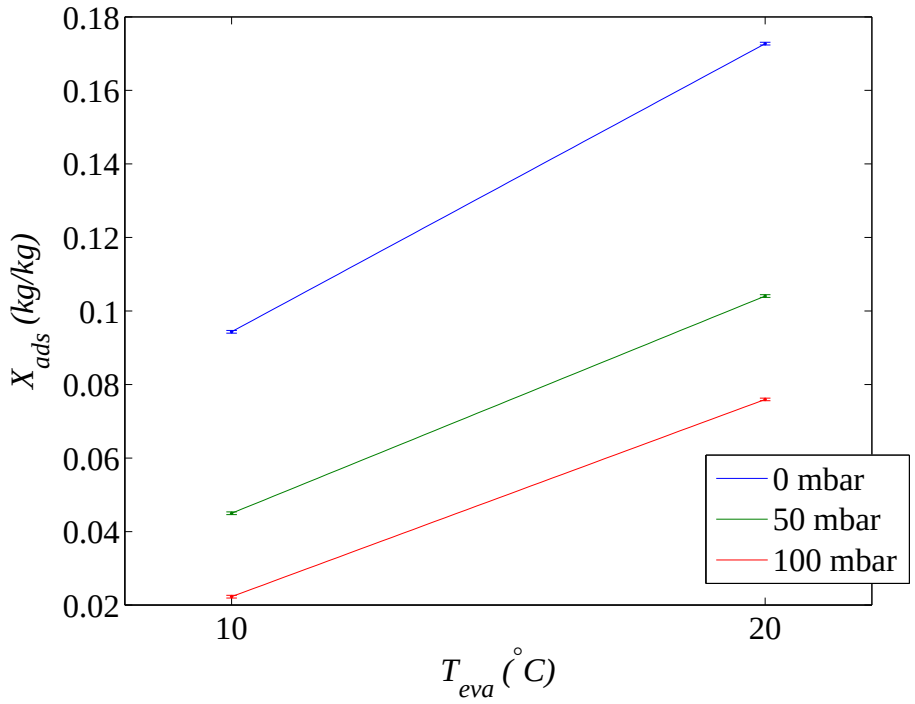

Figure 3.19: Adsorption capacity vs. Evaporator temperature graph for silica gel, 10°C, 20°C evaporator temperatures, 90°C-30°C adsorbent working temperatures.

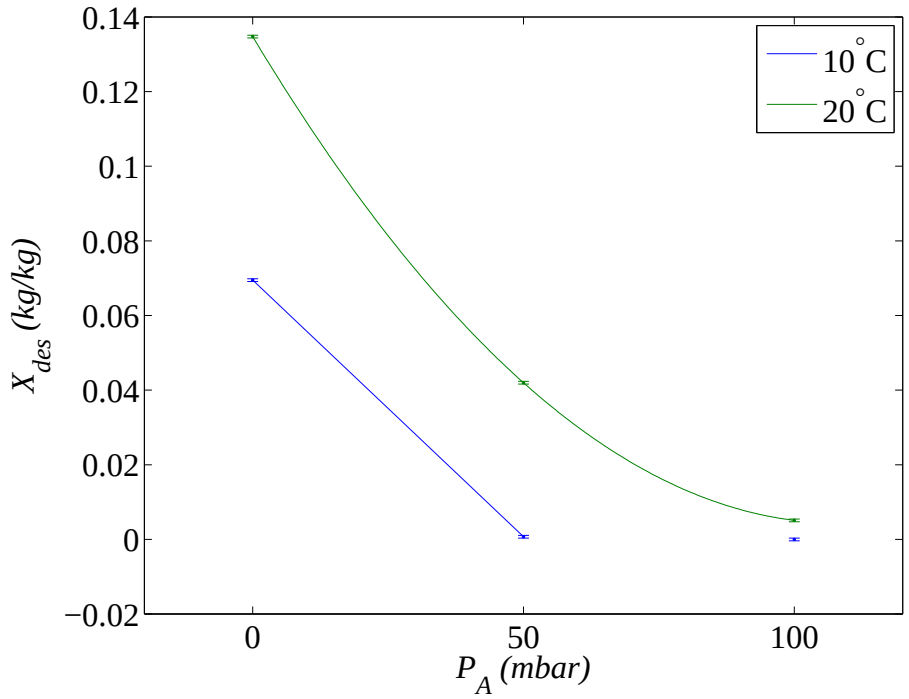

Figure 3.20: Desorption capacity vs. Residual air pressure graph for silica gel, 10°C, 20°C condenser temperatures, 90°C-30°C adsorbent working temperatures.

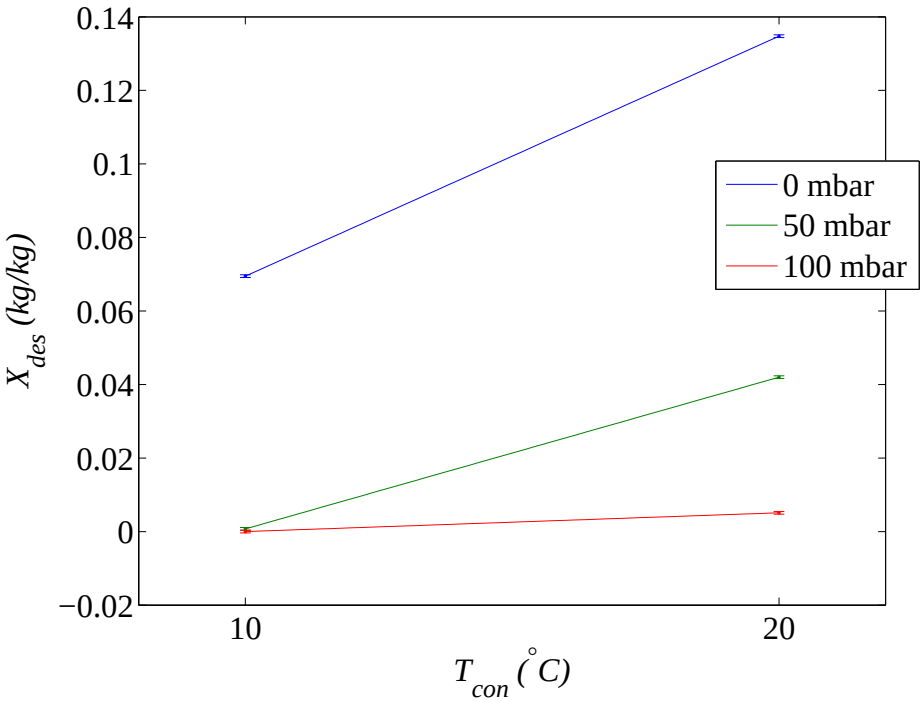

Figure 3.21: Desorption capacity vs. Condenser temperature graph for silica gel, 10°C, 20°C condenser temperatures, 90°C-30°C adsorbent working temperatures.

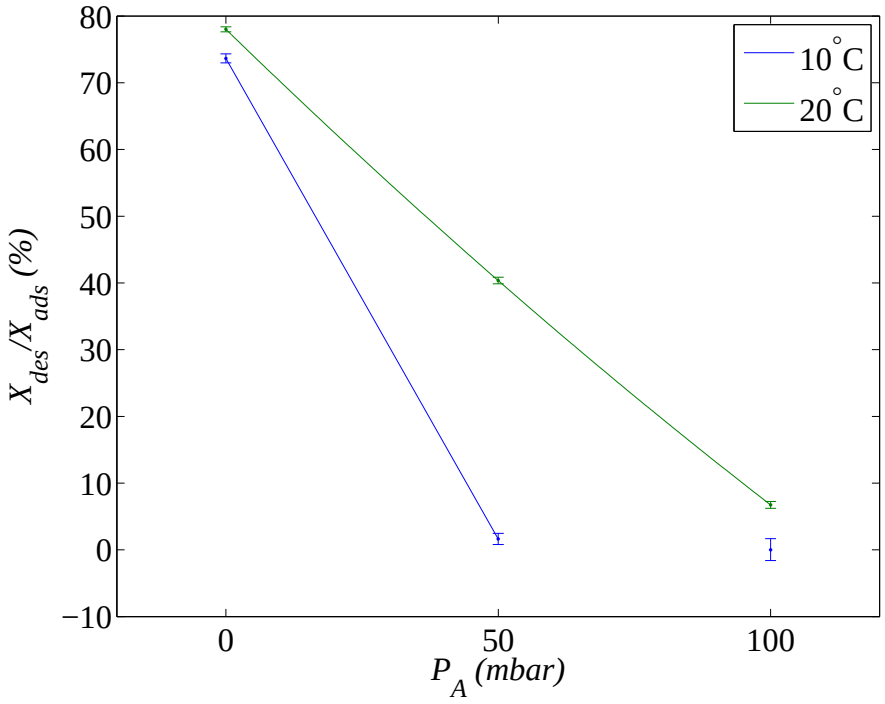

Figure 3.22: Ratio of desorption capacity to adsorption capacity vs. Residual air pressure graph for silica gel, 10°C, 20°C evaporator/condenser temperatures, 90°C-30°C adsorbent working temperatures.

3.2.2 Transient Effects on Adsorption

Changes in gas pressures over time are given in Figure 3.23 and Figure 3.24. Both cases showed a sudden initial decrease and increase pattern in pressure with a more lenient increase up to equilibrium pressure thereafter. Lower the residual air, sharper the decrease in pressure. These graphs show that most of the adsorption takes place in initial parts of the experiments. 20°C cases showed more erratic pressure patterns for 50 mbar case where evaporation/adsorption occured with a pulsating characteristic.

Much like gas pressure, gas temperature changes were characterized by a sudden decrease where tempereature minimas were at similar moments and continued by a slow increase to water bath temperature. Figure 3.25 and Figure 3.26 show these changes. Here, 20°C, 50 mbar case showed a different pattern than others as with the case of its gas pressure. This also implies that evaporation/adsorption was occured not in a continuous manner, but mostly with a pulsating manner with near instantenous

evaporation/adsorption moments at quick pressure/temperature drops.

Adsorbent temperature over time graphs are given in Figure 3.27 and Figure 3.28. As expected, experiments with lower residual air pressures yielded higher adsorbent temperatures. Hence, higher amount of adsorbed water. Maximas of temperatures occurred at relatively similar moments for all cases. Experiments with higher residual air reached equilibrium more quickly as amount of water adsorbed was lower. Pulsating adsorption pattern is also observable here for 20°C, 50 mbar case. Note that, pulses are also observed for 20°C, 0 mbar experiment, however they are both smaller in amplitude and quicker.

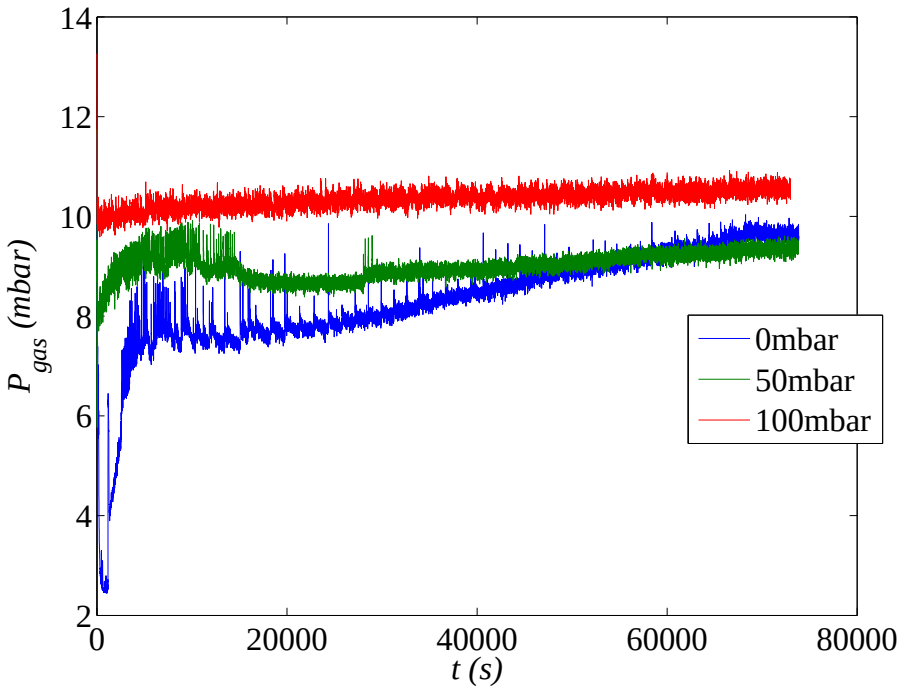

Figure 3.23: Gas pressure vs. Time graph of adsorption process for silica gel, 10°C evaporator temperature.

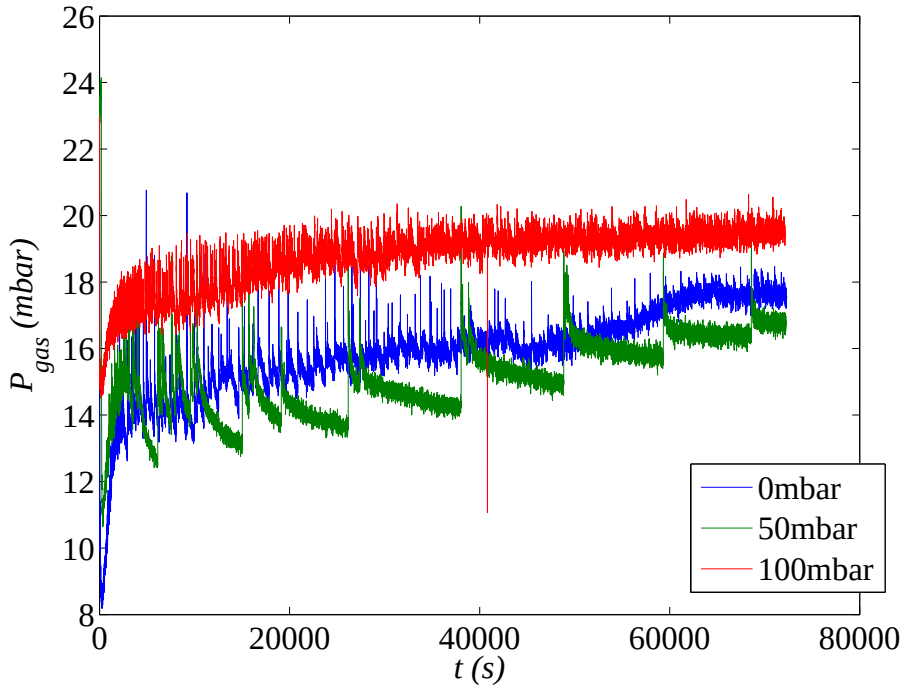

Figure 3.24: Gas pressure vs. Time graph of adsorption process for silica gel, 20°C evaporator temperature.

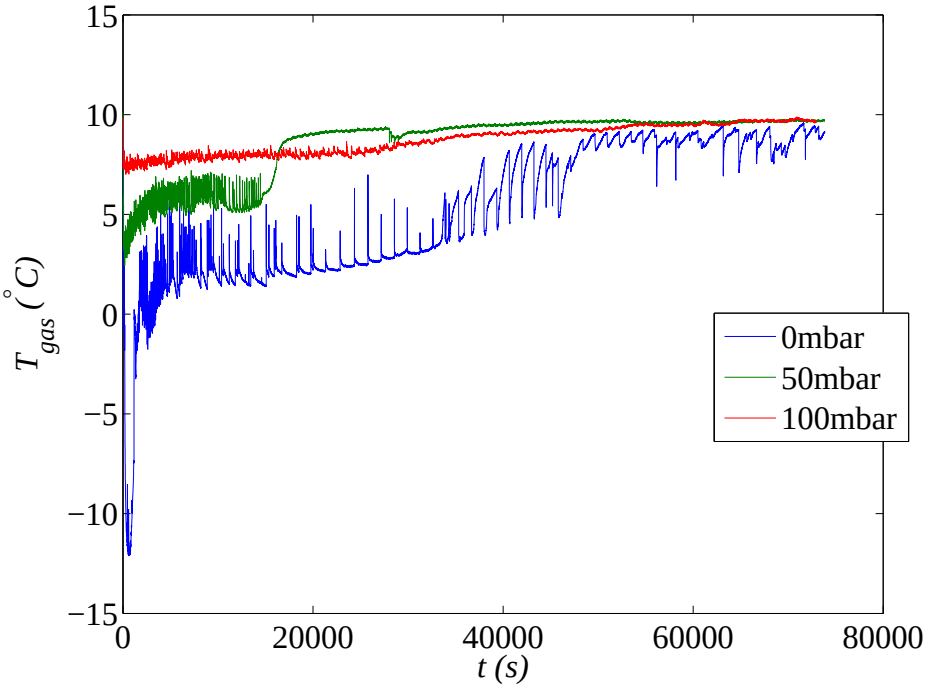

Figure 3.25: Gas temperature vs. Time graph of adsorption process for silica gel, 10°C evaporator temperature.

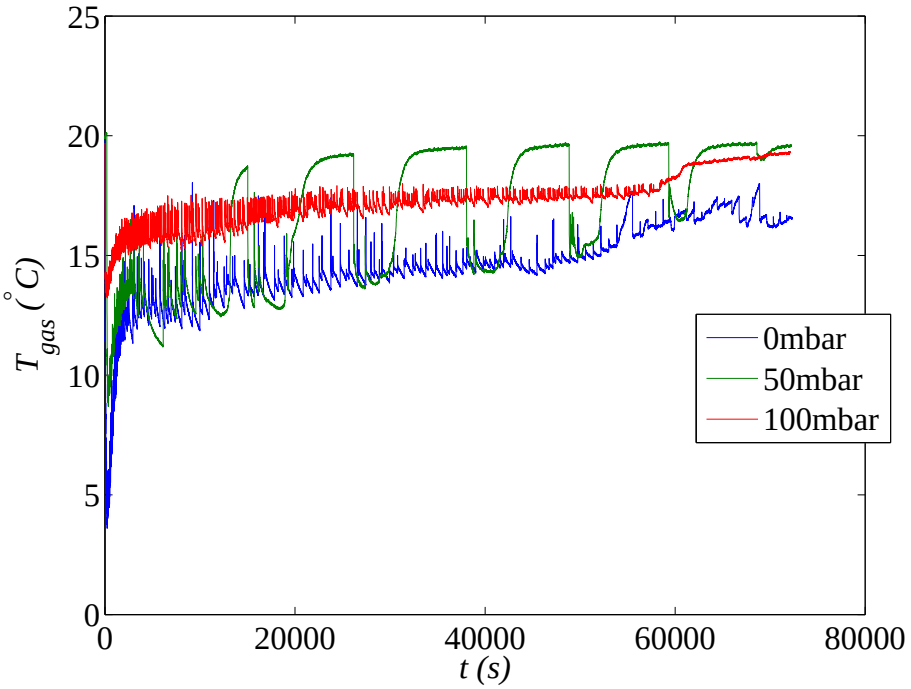

Figure 3.26: Gas temperature vs. Time graph of adsorption process for silica gel, 20°C evaporator temperature.

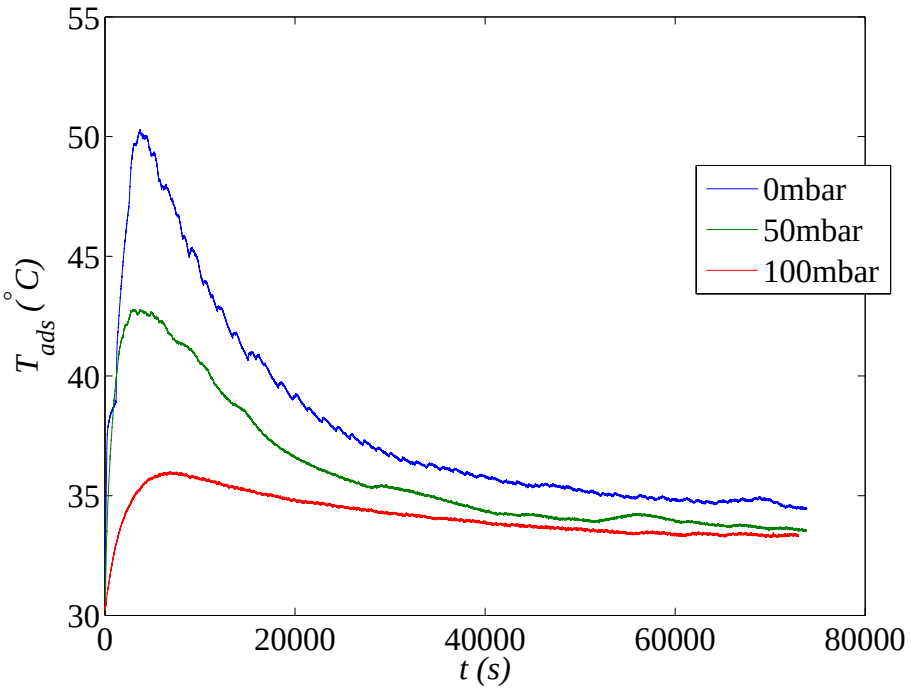

Figure 3.27: Average adsorbent temperature vs. Time graph of adsorption process for silica gel, 10°C evaporator temperature.

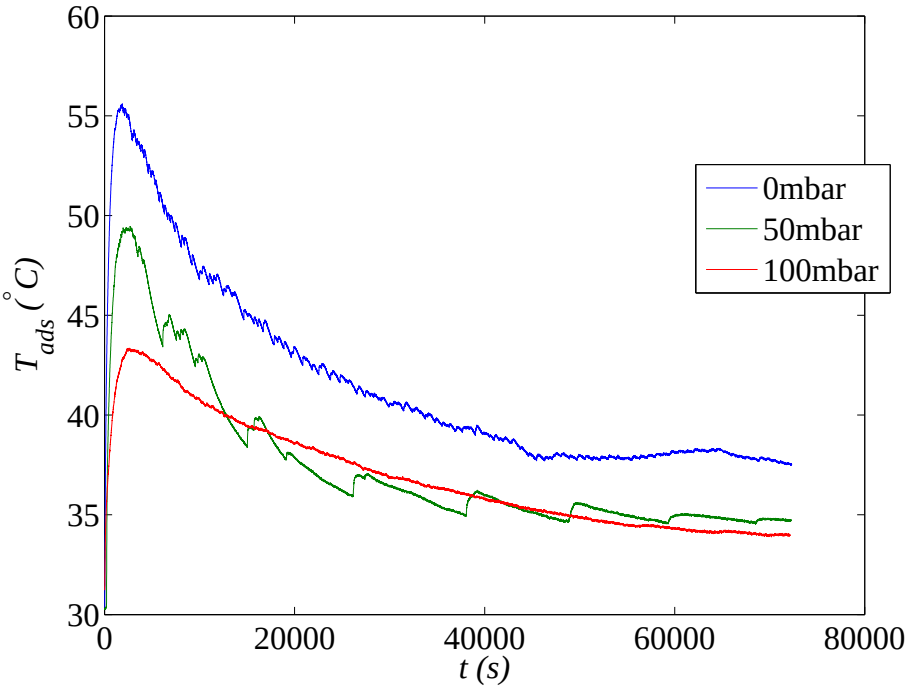

Figure 3.28: Average adsorbent temperature vs. Time graph of adsorption process for silica gel, 20°C evaporator temperature.

3.2.3 Transient Effects on Desorption

Gas pressure values in Figure 3.29 and Figure 3.30 showed a sudden decrease due to expansion and condensation and an almost constant value thereafter. Pressure values were significantly higher than the saturation pressure of condenser. As air within cannot create such high pressures by itself, part of vapor should had failed to condense. Experiments with lower residual air pressures showed larger pressure differences in the initial part of the experiments, implying that more vapor was condensed.

Desorbed amount of water had nearly reduced to zero at 50 mbar air pressure for 10°C condenser temperature, as mentioned in the previous section. This is also observable with the change in gas temperature in Figure 3.31 for that case as temperature change was almost identical to 100 mbar case, minimal change was logged. Thus, only minimal condensation occurs within the condenser. 100 mbar experiment for the same condenser temperature did not change at all. Hence, no condensation. Reaching the water bath temperature took longest among all adsorbents for most cases, especially

for 0 mbar cases, as amount of condensed water was large. Changes in gas temperature for 20°C condenser temperature are also observable in Figure 3.32.

Changes in adsorbent temperature over time are presented in Figure 3.33 and Figure 3.34. For 10°C case, it is seen that with 100 mbar air pressure, adsorbent temperature remained unchanged. This is expected as no water condensed within the condenser. In both condenser temperatures, 0 mbar cases were the earliest to reach equilibrium, except the 10°C, 100 mbar case where temperature was already at desorption temperature. 50 mbar cases for both condenser temperatures showed an almost constant temperature below the desorption temperature for the latter parts of the experiments. This may imply that there are still undesorbed water molecules on adsorbent which are slowly desorbing via heat taken from oven and carrying away that heat when molecule desorbs. This heat exchange may be the cause of the constant temperature regimes. Same phenomena was also observed for Zeolite 13X.

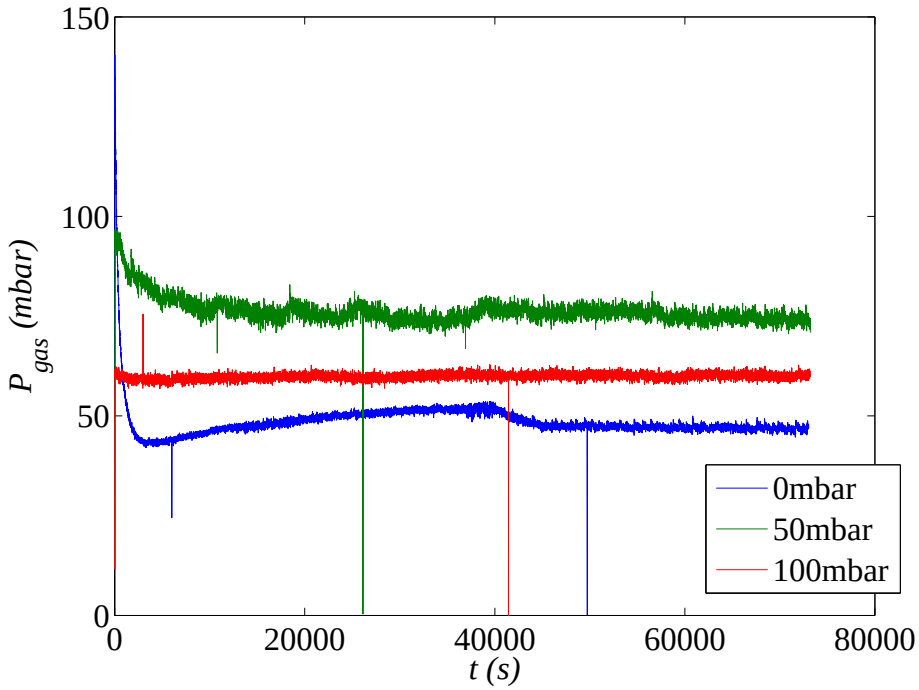

Figure 3.29: Gas pressure vs. Time graph of desorption process for silica gel, 10°C condenser temperature.

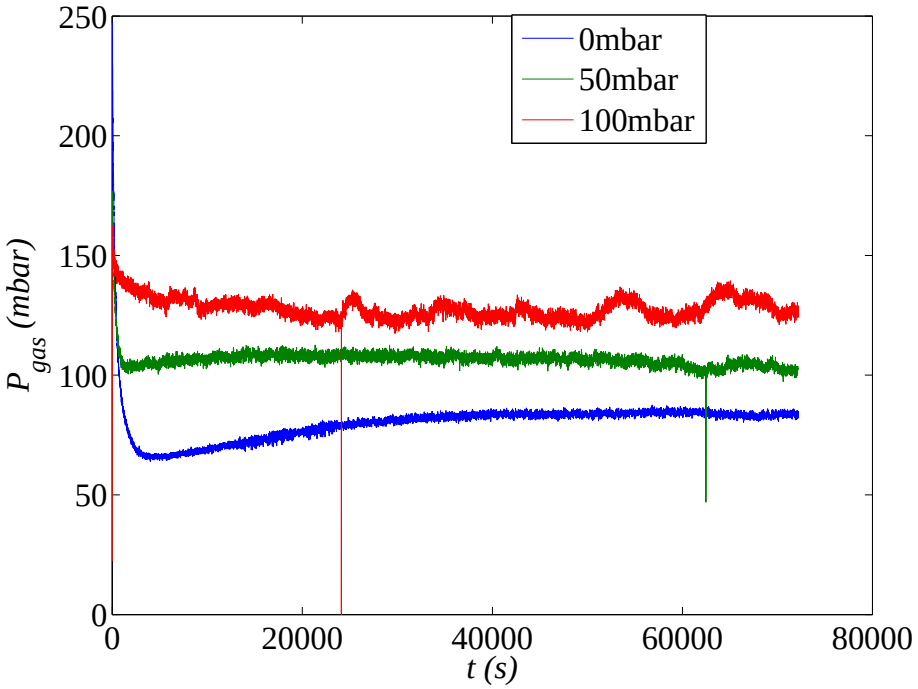

Figure 3.30: Gas pressure vs. Time graph of desorption process for silica gel, 20°C condenser temperature.

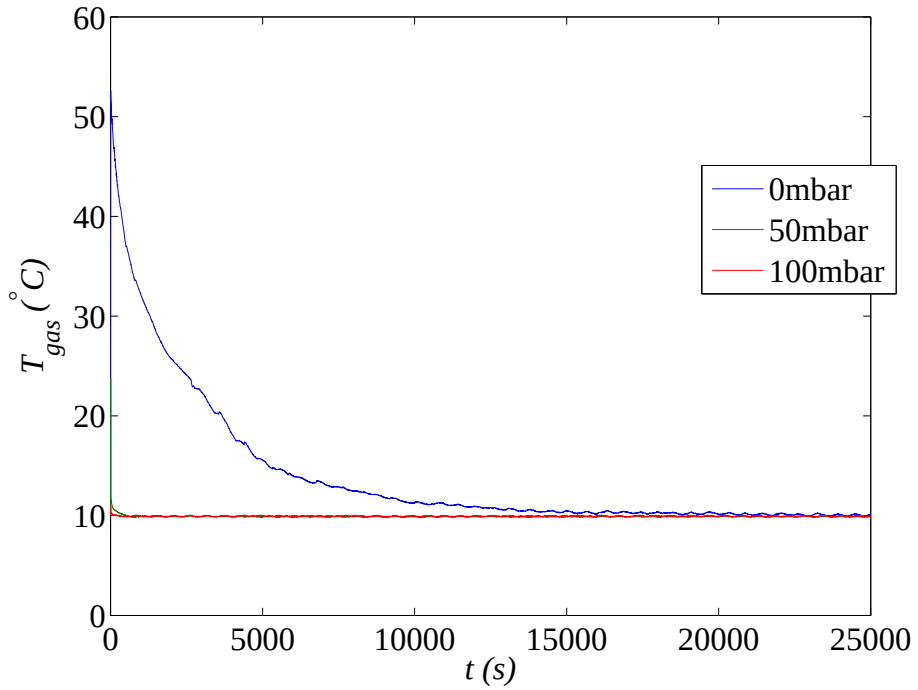

Figure 3.31: Gas temperature vs. Time graph of desorption process for silica gel, 10°C condenser temperature.

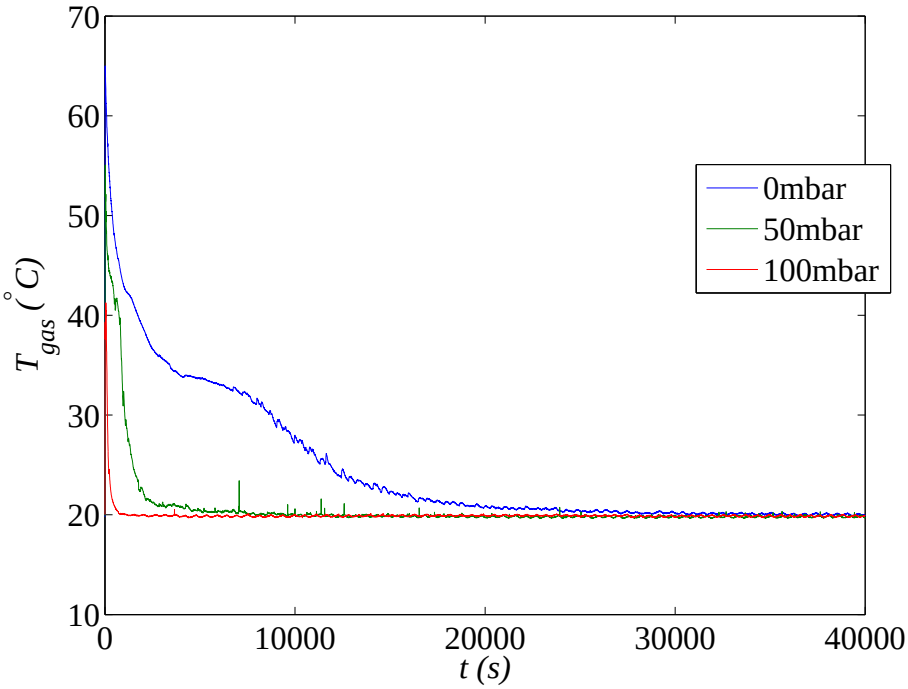

Figure 3.32: Gas temperature vs. Time graph of desorption process for silica gel, 20°C condenser temperature.

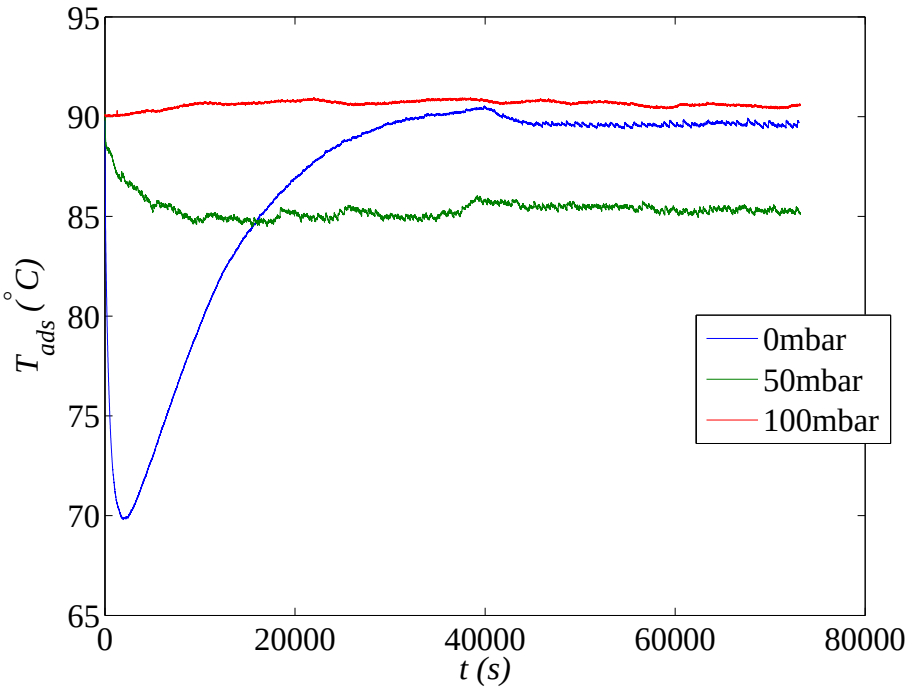

Figure 3.33: Average adsorbent temperature vs. Time graph of desorption process for silica gel, 10°C condenser temperature.

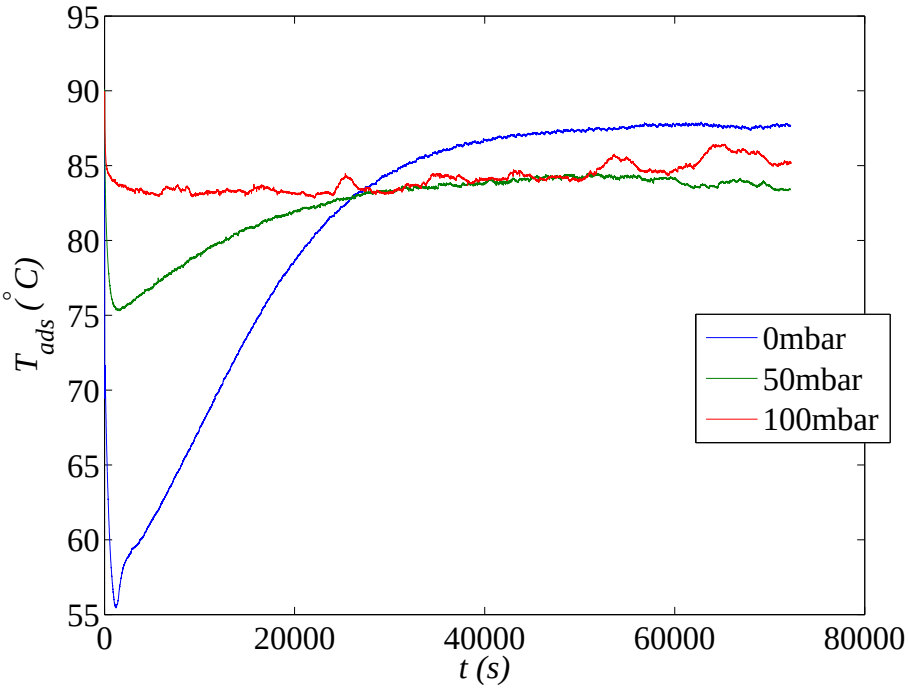

Figure 3.34: Average adsorbent temperature vs. Time graph of desorption process for silica gel, 20°C condenser temperature.

3.3 ZEOLITE 13X

For experiments with Zeolite 13X, a different approach was followed. Datas were taken not only at larger 160°C-40°C working temperatures, but also for smaller 140°C-115°C and 90°C-65°C working temperatures with smaller 0, 25 and 50 mbar air pressures. This way, not only the effects of residual air for different temperature regimes were investigated, change in adsorption capacities for 30°C evaporator/condenser temperature was also observed. Only 10°C evaporator/condenser temperature was investigated for 160°C-40°C and only 20°C for 90°C-65°C. 140°C-115°C case was investigated with all 10°C, 20°C and 30°C evaporator/condenser temperatures.

This adsorbent showed the lowest desorption capacities amongst all. Condensation within evaporator/condenser was only observed for 160°C-40°C working temperatures. No water was observed to be condensed for 140°C-115°C and 90°C-65°C experiments. Hence, no desorption data was included for them.

Equilibrium was not reached within the time frame of transient data range: around 20.5 hours. Therefore, transient datas should be treated as such.

3.3.1 Effects on equilibrium properties

For 160°C-40°C adsorbent and 10°C evaporator/condenser temperature case, we observe a logarithmic decay in both adsorption and desorption capacities in Table 3.8, Figure 3.35 and Figure 3.36; as well as desorption to adsorption capacity ratio in Table 3.9 and Figure 3.37 with increasing residual air values. Logarithmic decay in adsorption capacity was also observed for chemically similar natural zeolite. Reduction rates were relatively higher for desorption than adsorption, especially with 100 mbar residual air. As it can be seen, desorbed amount of water was the smallest among all adsorbents. Desorption capacities were not only small by itself, but also very small compared to adsorption capacities. This can also be seen in desorption to adsorption capacity ratios. Note that 50 mbar case showed almost similar ratio to 0 mbar case.

Table 3.8: Changes in adsorption and desorption capacities for Zeolite 13X, 10°C evaporator/condenser temperature, 160°C-40°C adsorbent working temperatures.

	10°C			
Residual air	X_{ads}	Reduction	X_{des}	Reduction
0 mbar	0.1026 ∓ 0.0004		0.0076 ∓ 0.0004	
50 mbar	0.0802 ∓ 0.0004	22%	0.0058 ∓ 0.0004	24%
100 mbar	0.0296 ∓ 0.0004	71%	0.0004 ∓ 0.0004	94%

Table 3.9: Desorption capacity to adsorption capacity ratios for Zeolite 13X, 10°C evaporator/condenser temperature, 160°C-40°C adsorbent working temperatures.

Residual air	10°C
0 mbar	7.4%
50 mbar	7.3%
100 mbar	1.5%

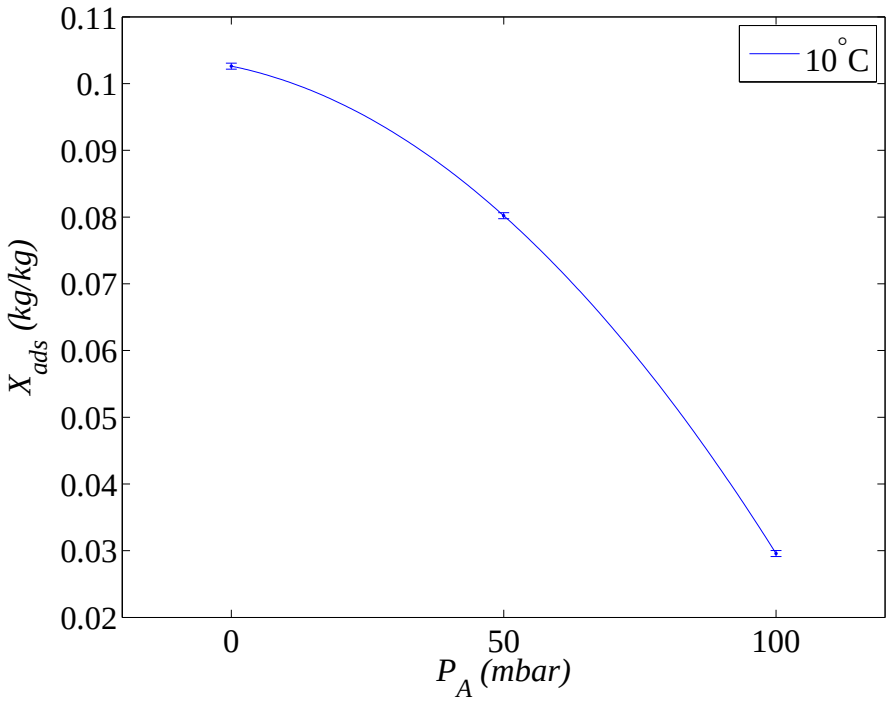

Figure 3.35: Adsorption capacity vs. Residual air pressure graph for Zeolite 13X, 10°C evaporator temperature, 160°C-40°C adsorbent working temperatures.

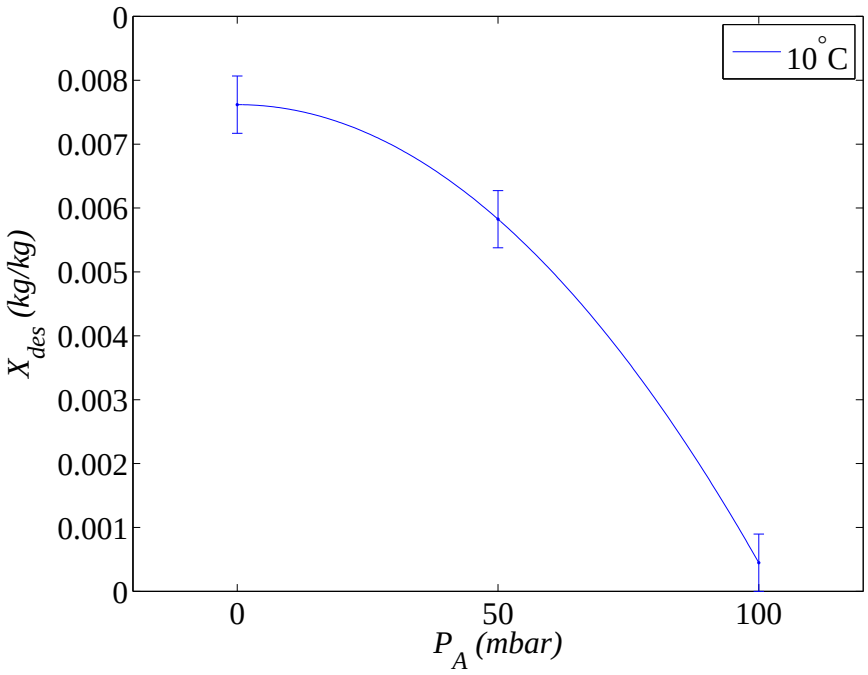

Figure 3.36: Desorption capacity vs. Residual air pressure graph for Zeolite 13X, 10°C condenser temperature, 160°C-40°C adsorbent working temperatures.

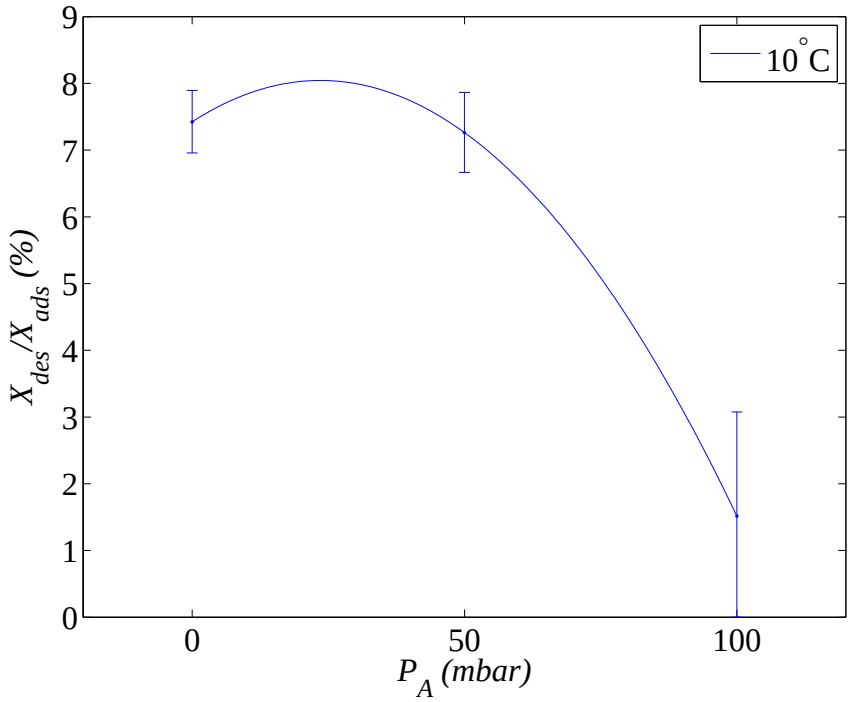

Figure 3.37: Ratio of desorption capacity to adsorption capacity vs. Residual air pressure graph for Zeolite 13X, 10°C evaporator/condenser temperature, 160°C-40°C adsorbent working temperatures.

For 140°C-115°C working temperatures whose datas are presented in Table 3.10, Figure 3.38 and Figure 3.39; it is seen that, with higher evaporator temperatures, reduction rates in adsorption capacities decrease. All experiments with same amount of residual air showed a logarithmic growth of adsorption capacity with increasing evaporator temperatures. 10°C and 20°C evaporator temperatures showed an almost linear decrease in adsorption capacities with increasing air pressures while 30°C case showed a characteristic logarithmic decay. Comparingly, at 20°C evaporator temperature, 90°C-65°C working temperature showed slightly less reduction in adsorption capacity than that of 140°C-115°C working temperature for the same evaporator temperature. This can be seen in Table 3.11 and comparatively in Figure 3.40.

Table 3.10: Changes in adsorption capacities for Zeolite 13X, 10°C, 20°C, 30°C evaporator temperatures, 140°C-115°C adsorbent working temperatures.

	10°C		20°C		30°C	
Residual air	X_{ads}	Red.	X_{ads}	Red.	X_{ads}	Red.
0 mbar	0.0193 ∓ 0.0004		0.0255 ∓ 0.0004		0.0277 ∓ 0.0004	
25 mbar	0.0108 ∓ 0.0004	44%	0.0201 ∓ 0.0004	21%	0.0259 ∓ 0.0004	6%
50 mbar	0.0036 ∓ 0.0004	81%	0.0134 ∓ 0.0004	47%	0.0165 ∓ 0.0004	40%

Table 3.11: Changes in adsorption capacities for Zeolite 13X, 20°C evaporator temperature, 90°C-65°C adsorbent working temperatures.

	20°C	
Residual air	X_{ads}	Reduction
0 mbar	0.0215 ∓ 0.0004	
25 mbar	0.0179 ∓ 0.0004	17%
50 mbar	0.0125 ∓ 0.0004	42%

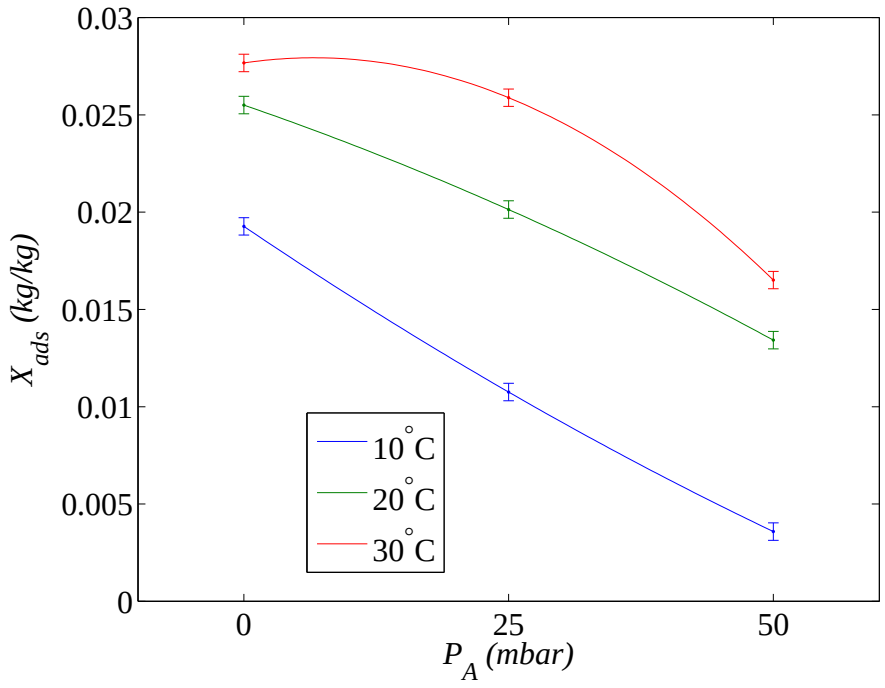

Figure 3.38: Adsorption capacity vs. Residual air pressure graph for Zeolite 13X, 10°C, 20°C, 30°C evaporator temperatures, 140°C-115°C adsorbent working temperatures.

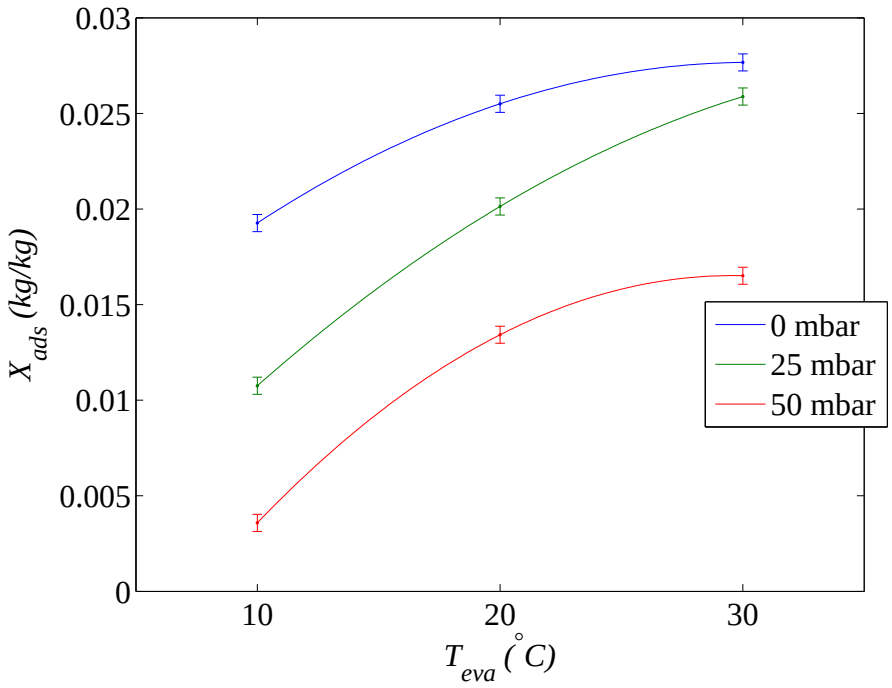

Figure 3.39: Adsorption capacity vs. Evaporator temperature graph for Zeolite 13X, 10°C, 20°C, 30°C evaporator temperatures, 140°C-115°C adsorbent working temperatures.

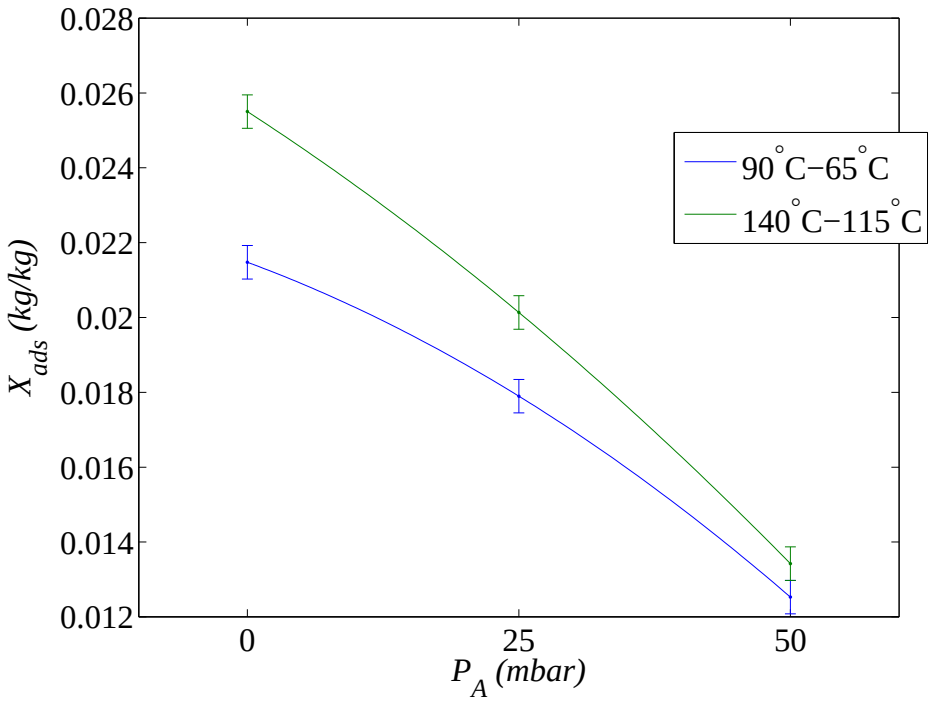

Figure 3.40: Adsorption capacity vs. Residual air pressure graph for Zeolite 13X, 20°C evaporator temperature, comparison between 140°C-115°C and 90°C-65°C adsorbent working temperatures.

3.3.2 Transient Effects on Adsorption

Only the datas of 160°C-40°C working temperatures were presented in this section. Note that during the experiment of 0 mbar residual air case, an ice sheet occurred at the top of waterline at earlier part of the experiment. This retarded the adsorption process, therefore those datas should be regarded as such.

Both 50 mbar and 100 mbar cases showed a steady linear increase in pressure with slope of the lesser air pressure being larger in Figure 3.41. Although ice sheet delayed the adsorption of 0 mbar case, it was still the one which reached higher pressures earliest. Thus, closer to equilibrium pressure.

Experiments with higher residual air pressures yielded lower changes in gas temperatures in Figure 3.42, which would effectively reduce the cooling power of adsorption machines. Very low temperatues was observed for 0 mbar case, well below the freezing point of water. This caused a layer of ice to form upon the waterline, halting the

evaporation for a time. Sudden increase and decreases were observed for al cases, indicating small pulses of adsorption. Note that, lower the residual air pressure was, less smooth the temperature datas were. Despite its higher adsorption capacity and occurance of ice layer, 0 mbar case was the first to reach a temperature close to that of water bath.

As expected, higher temperatures were observed for lower residual air pressures in Figure 3.43 due to higher adsorption capacities. Note that 0 mbar case was the one to reach to lower temperatures quickest. Hence, quickest to equilibrium. Datas were more chaotic for decreasing air pressures, probably due to slower nature of adsorption process.

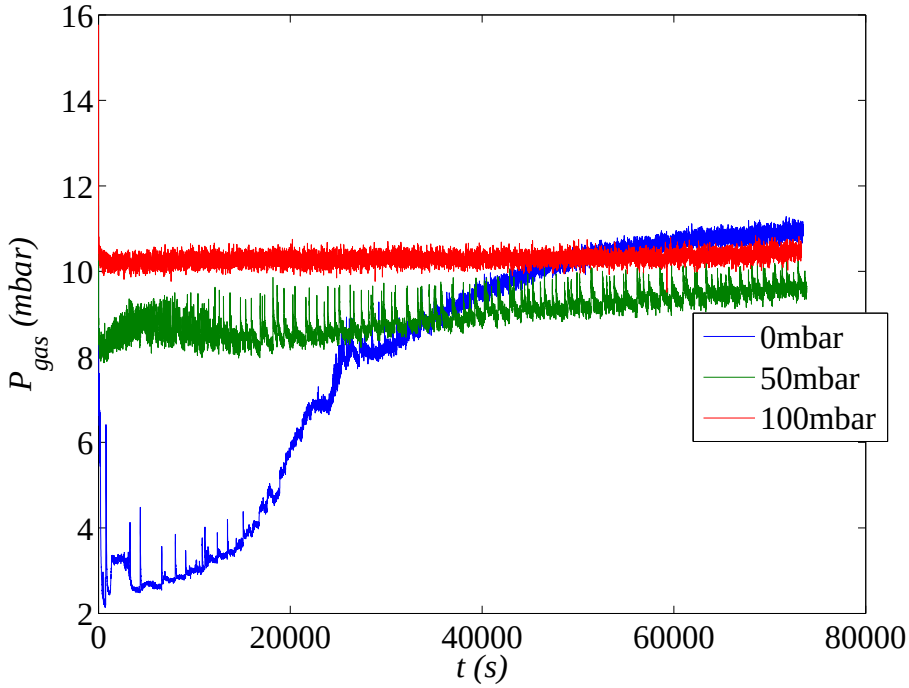

Figure 3.41: Gas pressure vs. Time graph of adsorption process for Zeolite 13X, 10°C evaporator temperature, 160°C-40°C adsorbent working temperatures.

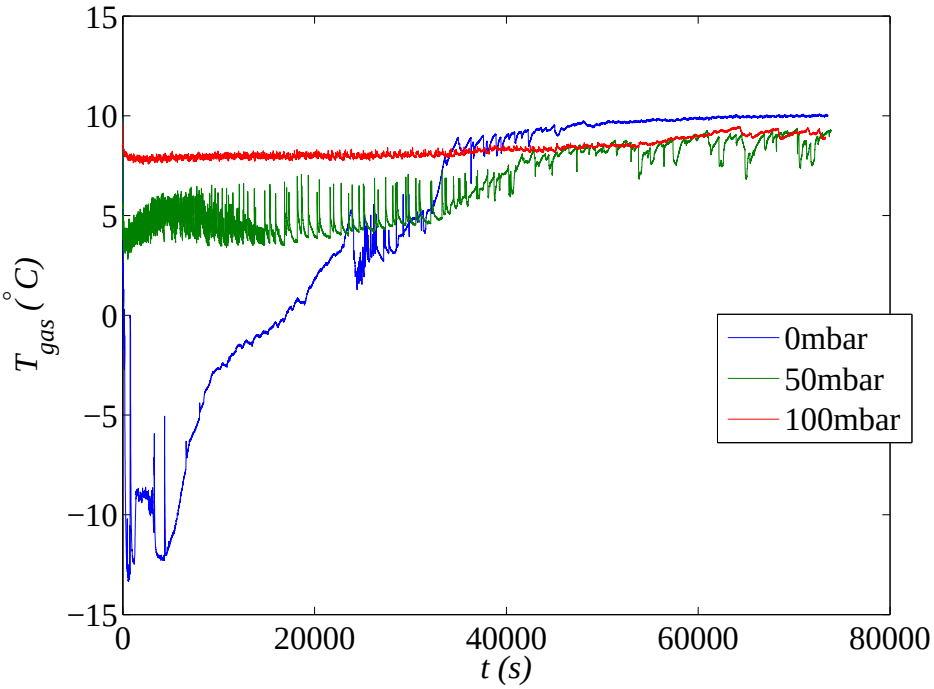

Figure 3.42: Gas temperature vs. Time graph of adsorption process for Zeolite 13X, 10°C evaporator temperature, 160°C-40°C adsorbent working temperatures.

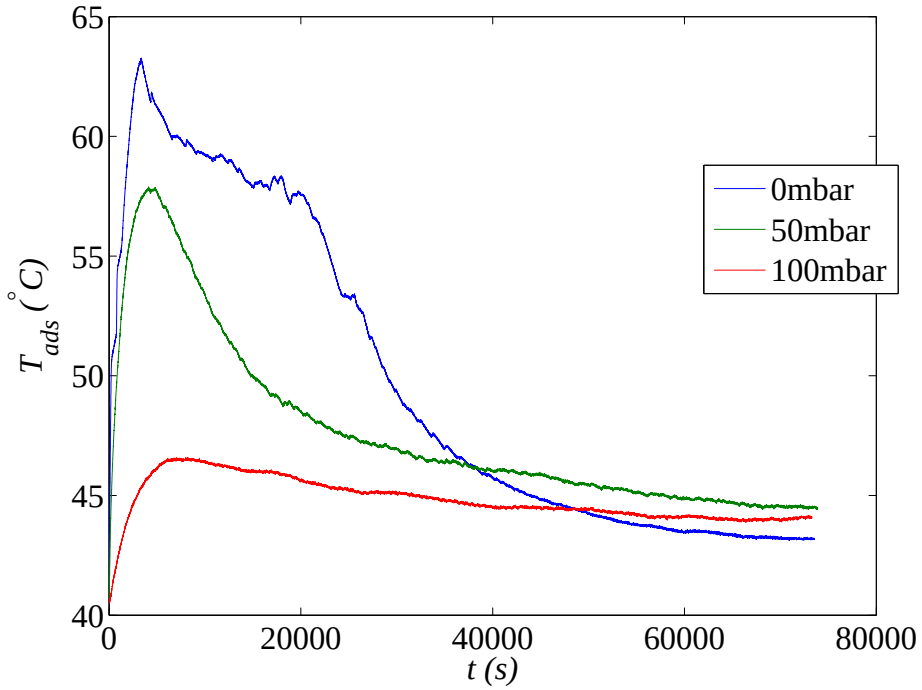

Figure 3.43: Average adsorbent temperature vs. Time graph of adsorption process for Zeolite 13X, 10°C evaporator temperature, 160°C-40°C adsorbent working temperatures.

3.3.3 Transient Effects on Desorption

Gas pressure changes in time were characterized by initial decreases due to condensation/expansion and more or less a constant value thereafter as seen on Figure 3.44. Lower the residual air pressure, higher the difference between starting pressure and final pressure was. Pressures higher than the saturation pressure of condenser means that some of the vapor lingers through oven and pipings and fails to condense in the condenser.

Among all desorption experiments, this particular adsorbent was the one whose gas temperatures reached to equilibrium fastest. This is observable in Figure 3.45. It was expected since Zeolite 13X had the lowest desorption capacities. All temperatures converged to water bath temperature around 2000^{th} second, a value far less than those of natural zeolite and silica gel.

Adsorbent temperatures were lower for lower residual air pressures, as seen on Figure 3.46. This means that experiments with lower residual air desorbed more water than others. Curves of 0 mbar and 50 mbar cases were particularly similar. While 100 mbar case showed a low drop in temperature with steady increase thoroughout, 0 mbar and 50 mbar cases converged to an almost constant temperature in the latter part of the experiments. This phenomena was also observed for silica gel for 50 mbar cases of both condenser temperatures, especially with 10°C condenser temperature. Here, it is even more remarkable. This may mean that some of the water remains still undesorbed on adsorbent and heat taken by desorbing water was roughly equal to heat obtained from the oven for sometime. This may be the case of the aforementioned constant temperature regime. 100 mbar case may lack such undesorbed water due to its low adsorption capacity. Hence, its steady increase in temperature. Reasons of this will be discussed in the conclusions section.

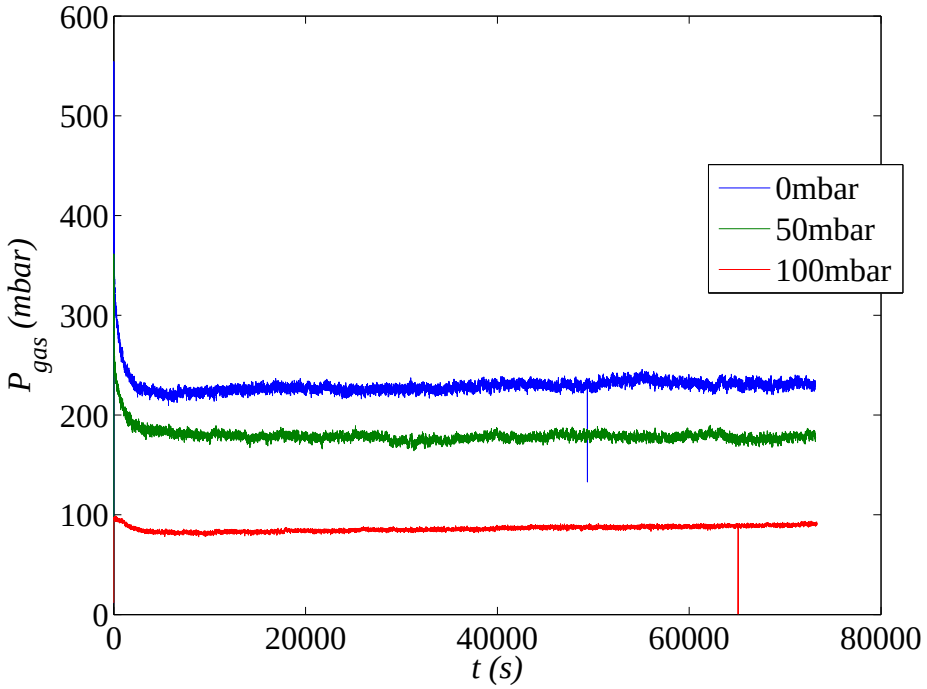

Figure 3.44: Gas pressure vs. Time graph of desorption process for Zeolite 13X, 10°C condenser temperature, 160°C-40°C adsorbent working temperatures.

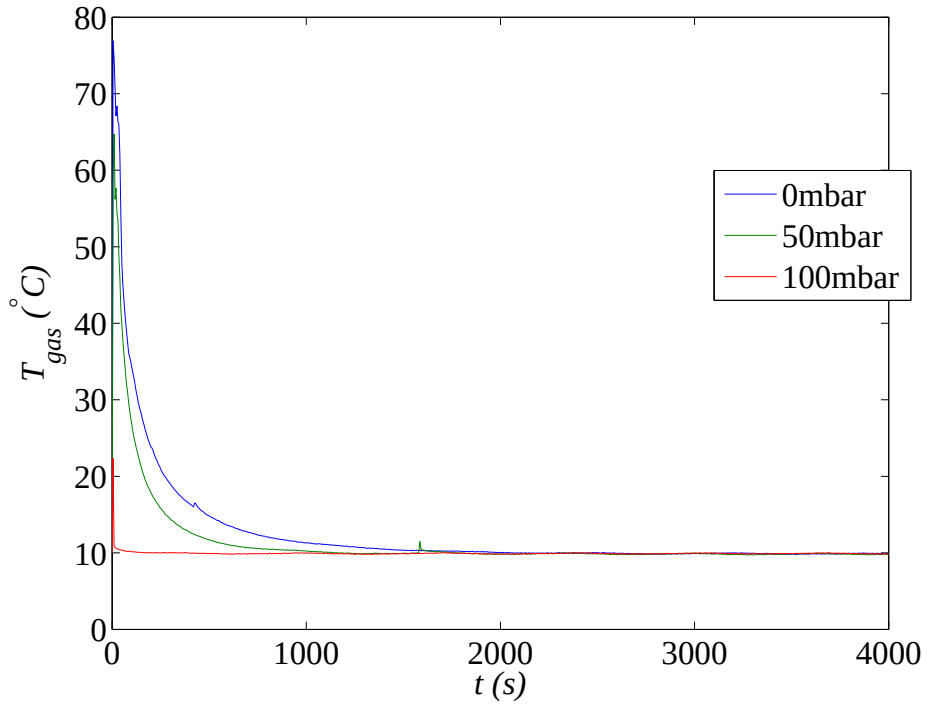

Figure 3.45: Gas temperature vs. Time graph of desorption process for Zeolite 13X, 10°C condenser temperature, 160°C-40°C adsorbent working temperatures.

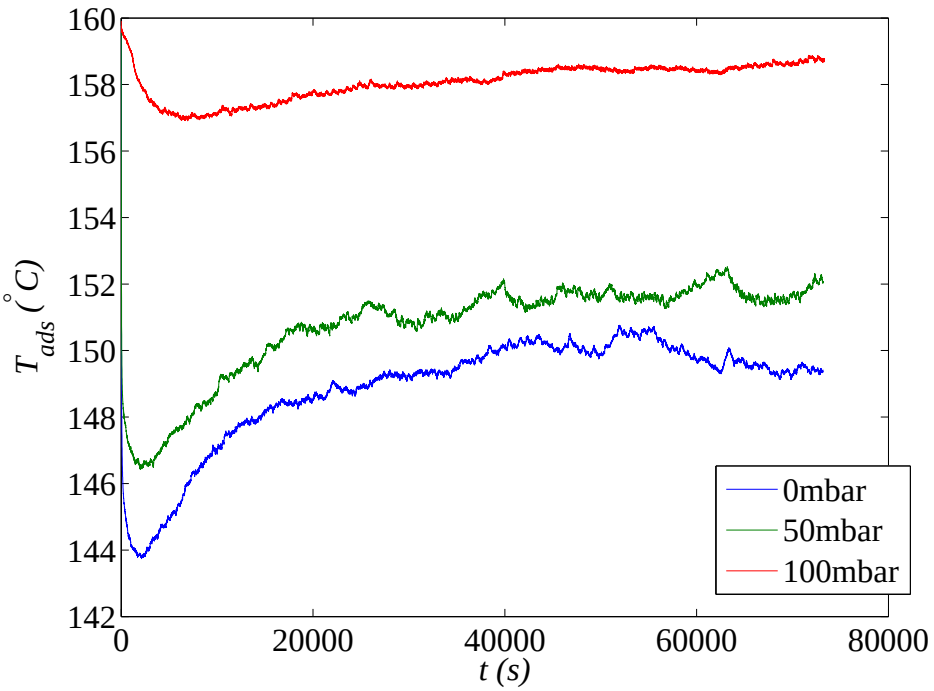

Figure 3.46: Average adsorbent temperature vs. Time graph of desorption process for Zeolite 13X, 10°C condenser temperature, 160°C-40°C adsorbent working temperatures.

CHAPTER 4

REMARKS, DISCUSSIONS AND CONCLUSIONS

Testing adsorption refrigeration with systematic amounts of injected air has revealed a variety of negative effects. Most important of such effects was the significant reductions in adsorption and desorption capacities. All cases, without exception, showed the aforementioned result with increasing amounts of residual air. Higher the amount of air was, larger the reductions were. That would negatively affect the cooling performance of an adsorption refrigerator or heating performance of a heat pump.

Universally, for all adsorbents, higher evaporator/condenser temperatures yielded lower reductions by percentage of no-air values in both adsorption and desorption for the same amount of residual air. One reason of this case may be due to higher mass diffusivity. Higher temperatures of vapor and air will result in higher mass diffusion rates. Therefore, water vapor may reach the grain pores they adsorbed on more effectively. However, by theory, a decrease in diffusivity would only retard the adsorption process, and should not affect the final equilibrium capacities. Stephan flux might also played a role during adsorption. Although it decreases diffusivity on grain pores, some pores might be clogged with air, essentially making them unavailable for adsorption. Diffusivity may however be the reason of decrease in desorption capacities. Higher mass diffusivity might had played a role in condensation, allowing vapor to better penetrate into condenser. Main reason behind lower adsorption capacities may be the ratio of partial air pressure to total pressure in the case of adsorption. As adsorption process comes to an end, total pressure reaches the equilibrium pressure: saturation pressure at the temperature of evaporator/condenser. As the saturation pressure increases, ratio of partial air pressure to that pressure will decrease.

For example, if we round and accept 12 mbar as saturation pressure of 10°C and 23 mbar of 20°C, ratio of a 7 mbar partial air pressure would be 58% for 10°C and 30% for 20°C. Hence, by ratio there will be more reduction in adsorbed vapor for lower evaporator/condenser temperatures. This phenomena can effectively reduce the final, equilibrium adsorption capacities, with lower the evaporator temperature, higher the reduction.

Condensed water within condenser was always lower than that of adsorbed, including no-air experiments. There may be several reasons for that. Part of this fact is due to the configuration of the experiment. This phenomena was also observed with a very similar experimental apparatus before, with no air involved [23]. Desorption was always characterized by sudden decreases in pressure due to expansion and condensation and more or less a constant regime thereafter. Logged final pressures were always much higher than the saturation pressures, including no-air experiments. Most, if not all of this pressure must be created by vapor, failing to condense. Inevitably, there would be temperature gradients between the hotter bed side and colder condenser side. As the position of the logging pressure sensor was closer to bed side than the thermocouple within condenser, higher pressures can be observed due to higher temperatures, different than that of corresponding vapor temperatures within condenser. Therefore, condenser might had reached to an equilibrium where further condensation does not occur, although logged pressure values were much higher than the saturation pressure. Vapor temperatures reached to their respective water bath temperatures relatively quickly, condensation after that period should only be minimal, if any. This was the reason why only adsorbent temperature and vapor temperature was taken into account for ending a desorption experiment. Difference between initial pressure value and final pressure value was lower for experiments with higher residual air. This indicates that, significant amounts of vapor did desorb but failed to condense due to the effects of air on condensation. Effect of residual air on barring the condensation is a well-known phenomena [27, 28, 29, 30, 31]. So, part of the reduction in the amount of water condensed in condenser is attributable to negative effects of air on condensation. This is also observable in the fact that desorption capacity to adsorption capacity ratio was always lower for higher residual air experiments. Therefore, condensed water was not only lower due to lower adsorption capacity of higher residual air cases,

but also due to the fact that residual air affects condensation. Another fact is the inherent failure of complete reversibility from adsorption to desorption. This was observed before, even with no air involved [38]. So, there might be undesorbed molecules on the adsorbent which may contribute to reductions in desorption capacities. These undesorbed molecules might also be the cause of peculiar constant average adsorbent temperature regimes.

Note that, pipeline was held at a lower temperature than desorption temperatures, especially significantly lower than the 160°C desorption temperature of zeolites. Temperature was controlled at one point on the pipeline, where it was at a constant 60°C. So, there may be differences in temperature on various parts of the pipeline. Those facts inevitably resulted in part of the water vapor to filmwise condense upon the inner part of the pipeline. As a result, this would reduce the amount of water condensed within the condenser. This was the main drawback of the experiments as desorption readings might be erroneous due to that fact. However, as pipeline temperature was controlled at the same temperature for all experiments, more or less the same temperature distribution is expected over the pipeline for all experiments. This would, in turn, result in more or less the same amount of vapor to condense on pipeline for all experiments. Therefore, this fact would render all desorption data to be comparable to each other as approximately same amount of vapor is expected to condense on pipeline for every desorption experiment.

A peculiar phenomenon is seen on the average adsorbent temperature over time graphs of silica gel and Zeolite 13X for desorption experiments. For some cases, especially with the ones with residual air, a constant temperature regime below the desorption temperature over a relatively large period of time was observed. As adsorbent is constantly taking heat from oven, it can be concluded that something is taking away that heat from the adsorbent. Hence, constant temperature regime. There may be several reasons for that. One reason is, as the gas expands after the opening of valve V-1, it cools down the adsorbent to a lower temperature. This may cause some of the desorbed vapor to be re-adsorbed again. After the re-adsorption, desorption of those water molecules may slowly take place by transfer of heat from oven. Eventually resulting in desorbing water taking away that heat with them. However, if this was the case, significant increases in adsorbent temperature should be observed just after

the initial drop-down due to heat of adsorption. In fact, for all experiments, temperatures continued to drop for a while after valve was opened. Another and a more realistic reason may be due to the fact that there were still undesorbed water upon adsorbent when valve was opened. This water eventually started to desorb after valve was opened and pressure was relieved, taking away heat with it in process. Presence of air can affect this process. Note that, for silica gel, 0 mbar cases were the ones which reached desorption temperature quickest. This retardation of desorption might be tied to the effect of Stephan flux. This flux might had created a layer of air upon grain pores of adsorbent, which increases the heat and mass transfer resistance on pores. However, air-rich layer was reported not to form for desorption. It was mentioned that, desorption rate was limited by the intraparticle vapor diffusion and heat transfer [38].

Concerning the adsorption capacities for larger desorption-adsorption temperature difference experiments, all adsorbents gave different results. Most importantly, zeolites showed a logarithmic decay with increasing air mass whereas silica gel showed an exponential decay. However, silica gel was also the most affected with the 50 mbar air case, adsorption capacity reduced further than zeolites. Among all adsorbents, a maximum of 82% of reduction was observed in adsorption capacity with 100 mbar of air for 10°C evaporator temperature for natural zeolite. Reduction in adsorption capacities reduced with increasing evaporator temperature. Highest reduction observed at 20°C was 56%, that of silica gel.

Reductions in adsorption capacity for 140°C-115°C desorption-adsorption temperature difference experiments of Zeolite 13X showed a gradual transition from logarithmic decay to a slight exponential one with decreasing evaporator temperature. As expected, higher evaporator temperatures showed lower reductions with increasing residual air due to reasons mentioned before. Comparing the performance of 140°C-115°C working temperature to lower 90°C-65°C at 20°C evaporator temperature, it is observable that adsorption capacities of 140°C-115°C case fell more sharply with increasing residual air. Although both cases possess same temperature difference, reductions differed with temperature range. Another observable fact was that, there was a significant difference in reduction of adsorption capacities between working temperatures of 160°C-40°C and 140°C-115°C for the same amount of 50 mbar air

and same 10°C evaporator temperature. Whereas 160°C-40°C case reduced 22%, 140°C-115°C case reduced 81%. A significant difference. This clearly shows that reduction in adsorption capacity is also a function of adsorbent working temperatures, with higher the difference, lower the reduction.

Concerning desorption, there was not a single characteristic curve of reduction for all adsorbents. Natural zeolite showed almost linear decay for 10°C and exponential decay for 20°C condenser temperature. These characteristics was also the same for desorption to adsorption capacity ratio. Silica gel also showed exponential decay in desorption capacity for 20°C condenser temperature, 10°C case however, reduced to near zero already at 50 mbar of air. Ratio of desorption to adsorption capacity for silica gel showed a linear decrease for 20°C. Zeolite 13X was different in that, both desorption capacity and its ratio to adsorption capacity decayed logarithmically. Note that, desorption capacities were significantly low for Zeolite 13X, including no-air case. Zeolite 13X showed the largest hysteresis. Silica gel's ratios of desorption to adsorption capacity were the largest for no-air case. However, it fell quickly with the presence of air. In fact, silica gel was the most affected adsorbent from the presence of air, in terms of desorption. Like the adsorption capacities, desorption capacities affected less with the increase of condenser temperatures. Decrease in ratio of desorption to adsorption capacity with increasing air mass was universal for all adsorbents. This effectively means that, desorption stages affected more than adsorption from the presence of increasing air. Hence, increase in hysteresis.

As mentioned before, there were not many investigations about the effect of air on adsorption. Among the observed phenomena, heat transfer reduced in a granulated adsorbent layer with the presence of residual air, effectively reducing the performance of an adsorption heat pump [35]. 50% reduction of evaporator and condenser heat rate was said to be occurred with 1–2% non-condensing gases [36]. Much like this work, Glaznev et al. (2010) conducted a systematic study on adsorption with ever increasing air pressures [38]. Uptake (instantenous adsorption capacity) curves were investigated for different adsorbents. However, this work used only loose grains of adsorbent without an evaporator with liquid water within. Instead, only vapor at corresponding saturation pressure (10°C evaporator temperature) was held within a canister and air was injected in it with certain amounts. Uptake values were then

calculated through ideal gas equation with pressure values obtained from sensors. As there was no evaporator, partial pressure of vapor gradually decreased as it was being adsorbed. Unlike our work, final vapor pressure was lower than the initial vapor pressure. There was no connection to a water filled evaporator which would supply vapor and hold the total pressure at a constant saturation pressure. In this work, all cases yielded equal final adsorption capacities, regardless of amount of air added. Adsorption rates, however, all retarded with increasing residual air. Hysteresis in desorption was also seen in this study, albeit it was only tested where no air was involved. Not all of the adsorbed water was desorbed.

Unlike the study of Glaznev et al. (2010), our apparatus was akin to a practical adsorption refrigerator/heat pump with large amounts of adsorbent used and a liquid filled evaporator/condenser. Apart from that, none of the mentioned studies above showed reductions in adsorption or desorption capacities with increasing amount of air. In comparison with Glaznev et al. (2010), a reason for that should be the method of providing vapor to adsorbent, as that study did not use an evaporator/condenser. Another reason may be the loose amount of adsorbent grains. This would effectively reduce intraparticle resistances to a minimum. Our work provided valuable datas as adsorption capacity will define the cooling capacity of an adsorbent and desorption capacity will define the amount of reversibility. Besides, our study also presented the evolution of gas and adsorbent temperatures over time, two of the defining characteristics of adsorption.

Adsorbents natural zeolite, silica gel and Zeolite 13X with water as the adsorbate were investigated with increasing amounts of air. This study showed that both adsorption and desorption processes were heavily affected with the presence of air. Final adsorption and desorption capacities were dropped significantly with up to 100 mbar pressure of air within a 2.13 meter length, 16 mm diameter pipeline. This will inevitably reduce the cooling capacity of an adsorption refrigerator or heating capacity of a heat pump. Higher evaporator/condenser temperatures yielded lower amounts of reduction. Therefore, appliances where a higher cooling temperature suffice would be less affected, like air-conditioning. A large difference between desorption and adsorption temperatures is also preferable as this case was less affected by the presence of same amount of air. Apart from water-air diffusion, processes may be affected

by a non-stationary air-rich layer over grains, creating extra mass and heat transfer resistances. Moreover, air can accumulate within particle pores, perhaps clog it. Adding an another layer of negative effect. Thus, many different processes are involved. Further experimental and mathematical studies should be done in this field especially in micrometric and nanometric scales. Careful degassing, vacuum drying and proper sealing should be done on an adsorption refrigerator/heat pump as only a small amount of air or other non-condensable (0.3-0.9% of atmospheric pressure) can drastically affect such devices operating at pressures below atmospheric pressure, like those working with water and methanol.

REFERENCES

[1] Ali Al-Alili, Yunho Hwang, and Reinhard Radermacher. Review of solar thermal air conditioning technologies. *International Journal of Refrigeration*, 39:4–22, March 2014.

[2] J. Steven Brown and Piotr A. Domanski. Review of alternative cooling technologies. *Applied Thermal Engineering*, 64(1–2):252–262, March 2014.

[3] Biplab Choudhury, Bidyut Baran Saha, Pradip K. Chatterjee, and Jyoti Prakas Sarkar. An overview of developments in adsorption refrigeration systems towards a sustainable way of cooling. *Applied Energy*, 104:554–567, April 2013.

[4] Mingxi Liu, Yang Shi, and Fang Fang. Combined cooling, heating and power systems: A survey. *Renewable and Sustainable Energy Reviews*, 35:1–22, July 2014.

[5] H. Z. Hassan and A. A. Mohamad. A review on solar-powered closed physisorption cooling systems. *Renewable and Sustainable Energy Reviews*, 16(5):2516–2538, June 2012.

[6] K. R. Ullah, R. Saidur, H. W. Ping, R. K. Akikur, and N. H. Shuvo. A review of solar thermal refrigeration and cooling methods. *Renewable and Sustainable Energy Reviews*, 24:499–513, August 2013.

[7] X. Q. Zhai and R. Z. Wang. A review for absorbtion and adsorbtion solar cooling systems in china. *Renewable and Sustainable Energy Reviews*, 13(6–7):1523–1531, August 2009.

[8] Ioan Sarbu and Calin Sebarchievici. Review of solar refrigeration and cooling systems. *Energy and Buildings*, 67:286–297, December 2013.

[9] Y. Taki, R. F. Babus'Haq, and S. D. Probert. Combined heat and power as a contributory means of maintaining a green environment. *Applied Energy*, 39(2):83–91, 1991.

[10] J. Deng, R. Z. Wang, and G. Y. Han. A review of thermally activated cooling technologies for combined cooling, heating and power systems. *Progress in Energy and Combustion Science*, 37(2):172–203, April 2011.

[11] Dechang Wang, Jipeng Zhang, Xiaoliang Tian, Dawei Liu, and K. Sumathy. Progress in silica gel–water adsorption refrigeration technology. *Renewable and Sustainable Energy Reviews*, 30:85–104, February 2014.

[12] D.C. Wang, Y.H. Li, D. Li, Y.Z. Xia, and J.P. Zhang. A review on adsorption refrigeration technology and adsorption deterioration in physical adsorption systems. *Renewable and Sustainable Energy Reviews*, 14(1):344–353, January 2010.

[13] L. A. Chidambaram, A. S. Ramana, G. Kamaraj, and R. Velraj. Review of solar cooling methods and thermal storage options. *Renewable and Sustainable Energy Reviews*, 15(6):3220–3228, August 2011.

[14] Daniel J. Miles and Sam V. Shelton. Design and testing of a solid-sorption heat-pump system. *Applied Thermal Engineering*, 16(5):389–394, May 1996.

[15] Francis Meunier. Adsorption heat powered heat pumps. *Applied Thermal Engineering*, 61(2):830–836, November 2013.

[16] Hasan Demir, Moghtada Mobedi, and Semra Ülkü. A review on adsorption heat pump: Problems and solutions. *Renewable and Sustainable Energy Reviews*, 12(9):2381–2403, December 2008.

[17] Carlos Infante Ferreira and Dong-Seon Kim. Techno-economic review of solar cooling technologies based on location-specific data. *International Journal of Refrigeration*, 39:23–37, March 2014.

[18] TEİAŞ. Türkiye elektrik enerjisi 10 yıllık üretim kapasite projeksiyonu (2012-2021), 2012.

[19] Napoleon Enteria and Kunio Mizutani. The role of the thermally activated desiccant cooling technologies in the issue of energy and environment. *Renewable and Sustainable Energy Reviews*, 15(4):2095–2122, May 2011.

[20] Yuriy I. Aristov. Challenging offers of material science for adsorption heat transformation: A review. *Applied Thermal Engineering*, 50(2):1610–1618, February 2013.

[21] Ahmed A. Askalany, Bidyut B. Saha, Keishi Kariya, Ibrahim M. Ismail, Mahmoud Salem, Ahmed H. H. Ali, and Mahmoud G. Morsy. Hybrid adsorption cooling systems–an overview. *Renewable and Sustainable Energy Reviews*, 16(8):5787–5801, October 2012.

[22] Todd Otanicar, Robert A. Taylor, and Patrick E. Phelan. Prospects for solar cooling – an economic and environmental assessment. *Solar Energy*, 86(5):1287–1299, May 2012.

[23] İsmail Solmuş, Cemil Yamalı, Bilgin Kaftanoğlu, Derek Baker, and Ahmet Çağlar. Adsorption properties of a natural zeolite–water pair for use in adsorption cooling cycles. *Applied Energy*, 87(6):2062–2067, June 2010.

[24] I.S. Glaznev and Yu.I. Aristov. Kinetics of water adsorption on loose grains of SWS-1l under isobaric stages of adsorption heat pumps: The effect of residual air. *International Journal of Heat and Mass Transfer*, 51(25–26):5823–5827, December 2008.

[25] W. Z. Nusselt. Surface condensation of water vapor. *Z. Ver. Deut. Ing.*, 60:541–546, 1916.

[26] David Al'bertovich Frank-Kamenetskii. *Diffusion and heat transfer in chemical kinetics*. Plenum Press, New York [etc.], 1969.

[27] J.W. Rose. Condensation of a vapour in the presence of a non-condensing gas. *International Journal of Heat and Mass Transfer*, 12(2):233–237, February 1969.

[28] V.E Denny and V.J Jusionis. Effects of noncondensable gas and forced flow on laminar film condensation. *International Journal of Heat and Mass Transfer*, 15(2):315–326, February 1972.

[29] Barbara Mazzarotta and Enzo Sebastiani. Process design of condensers for vapor mixtures in the presence of non-condensable gases. *The Canadian Journal of Chemical Engineering*, 73(4):456–461, 1995.

[30] Seungmin Oh and Shripad T. Revankar. Experimental and theoretical investigation of film condensation with noncondensable gas. *International Journal of Heat and Mass Transfer*, 49(15–16):2523–2534, July 2006.

[31] Jun-De Li, Mohammad Saraireh, and Graham Thorpe. Condensation of vapor in the presence of non-condensable gas in condensers. *International Journal of Heat and Mass Transfer*, 54(17–18):4078–4089, August 2011.

[32] A.P. Burdukov, N.S. Bufetov, N.P. Deriy, A.R. Dorokhov, and V.I. Kazakov. EXPERIMENTAL STUDY OF THE ABSORPTION OF WATER VAPOR BY THIN FILMS OF AQUEOUS LITHIUM BROMIDE. *Heat transfer. Soviet research*, 12(3):118–123, 1980.

[33] F. Cosenza and G. C. Vliet. Absorption in falling water/LiBr films on horizontal tubes. *ASHRAE Transactions*, 96:693–701, 1990.

[34] V. P. Vorotilin and L. I. Heifets. Chemical industry. In *Chemical Industry*, pages 502–506. 8 edition, 1987.

[35] L. I. Heifets, D. M. Predtechenskaya, Y. V. Pavlov, and B. N. Okunev. Modeling of the dynamic effects in the adsorbent beds. 1. simple method of estimation of thermal conductivity of the composite adsorbent bed (CaCl2 impregnated into pores of silicagel lattice). *Moscow University Chemistry Bulletin*, 47(4):274, 2006.

[36] Michael A. Lambert. Design of solar powered adsorption heat pump with ice storage. *Applied Thermal Engineering*, 27(8–9):1612–1628, June 2007.

[37] G. Restuccia, A. Freni, S. Vasta, and Yu Aristov. Selective water sorbent for solid sorption chiller: experimental results and modelling. *International Journal of Refrigeration*, 27(3):284–293, May 2004.

[38] Ivan Glaznev, Daniil Ovoshchnikov, and Yuriy Aristov. Effect of residual gas on water adsorption dynamics under typical conditions of an adsorption chiller. *Heat Transfer Engineering*, 31(11):924–930, 2010.

[39] K. C. Ng, H. T. Chua, C. Y. Chung, C. H. Loke, T. Kashiwagi, A. Akisawa, and B. B. Saha. Experimental investigation of the silica gel–water adsorption isotherm characteristics. *Applied Thermal Engineering*, 21(16):1631–1642, November 2001.

[40] Yuri I. Aristov, Mikhail M. Tokarev, Angelo Freni, Ivan S. Glaznev, and Giovanni Restuccia. Kinetics of water adsorption on silica fuji davison RD. *Microporous and Mesoporous Materials*, 96(1–3):65–71, November 2006.

[41] Kakiuchi H, Shimooka S, Iwade M, Oshima K, Yamazaki M, Terada S, Watanabe H, and Takewaki T. Water vapor adsorbent FAM-z02 and its applicability to adsorption heat pump. *KAGAKU KOGAKU RONBUNSHU*, 31(4):273–277, 2005.

[42] B.N. Okunev, A.P. Gromov, V.L. Zelenko, I.S. Glaznev, D.S. Ovoshchnikov, L.I. Heifets, and Yu.I. Aristov. Effect of residual gas on the dynamics of water adsorption under isobaric stages of adsorption heat pumps: Mathematical modelling. *International Journal of Heat and Mass Transfer*, 53(7–8):1283–1289, March 2010.

[43] İsmail Solmuş, Bilgin Kaftanoğlu, Cemil Yamalı, and Derek Baker. Experimental investigation of a natural zeolite–water adsorption cooling unit. *Applied Energy*, 88(11):4206–4213, November 2011.